



---

## OSTM/Jason-2 Products Handbook

---

---

### References:

CNES : SALP-MU-M-OP-15815-CN  
EUMETSAT : EUM/OPS-JAS/MAN/08/0041  
JPL : OSTM-29-1237  
NOAA/NESDIS : Polar Series/OSTM J400  
Issue: 2 rev 0

Date: Apr 15<sup>th</sup>, 2025

---



**Chronology Issues:**

Issue:	Date:	Reason for change:
1rev0	June 17, 2008	Initial Issue
1rev1	July 31, 2008	Adding NOAA doc id, JASON2 launch date, and correction of SSH, SLA terms
1rev2	November 28, 2008	Update for the OGDR data distribution to users (inline with product version 'c').
1rev3	January 20, 2009	Update for the IGDR data distribution to users and adding the information included in document 'Access_to_Jason-2_data'
1rev4	August 3, 2009	Update for the GDR data distribution to users and of the editing procedure
	October 14, 2009	Introduction of the document in configuration management process at 4-partners level (Change request SALP-FT-7147).
1rev5	November 15 <sup>th</sup> , 2010	4 partner change request #7365 Correction on BUFR filenames; update of the Jason-2 BUFR descriptor sequence number' (e.g. from 005 to 010)
1rev6	January 13 <sup>th</sup> , 2001	4 partner change request #7974 : Location indicator in upper case for BUFR filenames
1rev7	September 9 <sup>th</sup> , 2011	Update to take into account version 'd' product (Change request SALP-FT-7233 and SALP-FT-8014)
1rev8	December 1 <sup>st</sup> , 2011	4-partner change request #8346 : <ul style="list-style-type: none"> <li>- New Mean Sea Surface: MSS_CNES-CLS-2011</li> <li>- New Mean Dynamic Topography : MDT_CNES-CLS-2009</li> <li>- Documentation update (new table on GDR-D orbit, new MSS&amp;MDT, etc.)</li> </ul> 4-partner change request #8379 : Implementation of NetCDF extension (.nc) on all Jason-2 level 2 products filenames (OGDR and OGDR-SSHA, IGDR, IGDR-SSHA and S-IGDR, GDR, GDR-SSHA and S-GDR)
1rev9	May 13 <sup>rd</sup> , 2015	<ul style="list-style-type: none"> <li>- Modification of the AVISO+ contact/address.</li> <li>- Correction on information given on tides models and load tides.</li> <li>- Update of NRT &amp; offline data access for NOAA.</li> </ul> 4-partner change request #10022 : Modification of orbit information to take into account the operational change to MOE and POE at "GDR-E" orbit standard.
1rev10	October 17 <sup>th</sup> , 2016	- Modification of orbit paragraph to introduce OSTM/Jason-2 interleaved orbit (SALP-FT-10555).



**Chronology Issues:**

Issue:	Date:	Reason for change:
1rev11	13 January 2017	<ul style="list-style-type: none"> <li>- Modification of GDR latency after OSTST 2016 recommendation. Latency extended from 60 to 90 days in order to allow cold sky calibration processing and use in radiometer calibrations. (SALP-FT-10763).</li> <li>- Update of Jason-2 orbit parameters (SALP-FT-10563).</li> </ul>
1rev12	15 July 2018	<ul style="list-style-type: none"> <li>- Transfer to LRO (SALP-FT-10947)</li> <li>- Jason-2 specifications updates associated to the transfer to interleaved LRO (SALP-FT-11282)</li> </ul>
1rev13	23 July 2019	<ul style="list-style-type: none"> <li>- SALP-FT-10176: Add reference to Altitude Grid in xref_meteorological_files</li> <li>- SALP-FT-11281: Implementation of a DORIS + GPS MOE orbit solution</li> </ul>
2rev0	15 Apr 2025	<ul style="list-style-type: none"> <li>- GDR-F Standard (SALP-FT-12220, SALP-FT-12386, SALP-FT-12663, SALP-FT-12931, SALP-FT-12933, SALP-FT-13059, SALP-FT-13256, SALP-FT-13328, SALP-FT-13544)</li> </ul>

**Document originally written by :**

J.P. DUMONT	CLS	
V. ROSMORDUC	CLS	
L. CARRERE	CNES	
N. PICOT	CNES	
C. MARECHAL	CNES	
A. COUHERT	CNES	
S. DESAI	NASA/JPL	
R. SCHARROO	EUMETSAT	
E. LEULIETTE	NOAA	

**People involved in this issue:**

F. BIGNALET-CAZALET	CNES	Date : Apr 15 <sup>th</sup> , 2025 <i>Francois Bignalet-Cazalet</i>
---------------------	------	--



## List of tables and figures

### List of tables:

<b>Table 1.</b> Differences between Auxiliary Data for O/I/GDR Products	1
<b>Table 2.</b> Summary of operational, interim, and final geophysical data record products (O/I/GDR) from the Jason-2 / Ocean Surface Topography Mission (OSTM).	2
<b>Table 3 :</b> Summary of error budget at the end of the verification phase	9
<b>Table 4 :</b> Main features of the OSTM/Jason-2 satellite	11
<b>Table 5.</b> Mean classical orbit elements	15
<b>Table 6 :</b> Orbit auxiliary data	15
<b>Table 7 :</b> Equator Crossing Longitudes (in order of Pass Number)	17
<b>Table 8 :</b> Equator Crossing Longitudes (in order of Longitude)	18
<b>Table 9 :</b> Equator Crossing Longitudes (in order of Pass Number)	20
<b>Table 10 :</b> Equator Crossing Longitudes (in order of Longitude)	21
<b>Table 11 :</b> Models and standards (Jason-2 GDR Product Version "T" and O/IGDR Product Version "c")	27
<b>Table 12 :</b> Version "d" models and standards	29
<b>Table 13.</b> GDR-C/GDR-D orbit standard	34
<b>Table 14 :</b> MSS_CNES-CLS11 model characteristics	35
<b>Table 15 :</b> MSS_CNES_CLS15 model characteristics	35
<b>Table 16 :</b> MDT_CNES-CLS09 model characteristics	37
<b>Table 16 :</b> Recommended editing criteria	42
<b>Table 17 :</b> Recommended filtering criteria	42
<b>Table 18 :</b> Main characteristics of (O)(I)GDR products	60
<b>Table 19 -</b> Dimensions used in the OSTM/Jason-2 data sets	61
<b>Table 20 -</b> netCDF variable type	61
<b>Table 21 -</b> Variable's attributes	61

### List of figures:

<b>Figure 1 :</b> Altimetric distances - Altitude, Range and Height	5
<b>Figure 2 :</b> OSTM/Jason-2 satellite (main components and artist view)	10
<b>Figure 3 :</b> OSTM/Jason-2 Posidon-3 Instrument	11
<b>Figure 4 :</b> OSTM/Jason-2 AMR Instrument and Antenna	12
<b>Figure 5 :</b> OSTM/Jason-2 DORIS Receiver Antenna and Instrument	12
<b>Figure 6 :</b> OSTM/Jason-2 Laser Reflector Array	13
<b>Figure 7 :</b> OSTM/Jason-2 Precision GPS Receiver	13
<b>Figure 8 :</b> OSTM/Jason-2 CARMEN-2 Instrument	14
<b>Figure 9 :</b> OSTM/Jason-2 LPT	14
<b>Figure 10 :</b> OSTM/Jason-2 T2L2 Optics Unit	14



# OSTM/Jason-2 Products Handbook

Iss :2.0 - date : Apr 15<sup>th</sup> , 2025



i.4

---

<b>Figure 11</b> : T/P, Jason-1 and OSTM/Jason-2 ground track coverage every 10 days	<b>15</b>
<b>Figure 12</b> : Mean Sea Surface MSS_CNES-CLS11.	<b>35</b>
<b>Figure 13</b> : Mean Sea Surface MSS_CNES_CLS15.	<b>35</b>
<b>Figure 14.</b> Mean Dynamic Topography MDT_CNES-CLS09	<b>37</b>
<b>Figure 14</b> : EGM96 geoid	<b>37</b>
<b>Figure 15</b> : Data set availability per product	<b>60</b>



## Applicable documents / reference documents

- AD 1 :** OSTM/Jason-2 System Requirements  
**TP3-J0-STB-44-CNES**
- AD 2 :** OSTM/Jason-2 Science and Operational Requirements  
**TP3-J0-SP-188-CNES**
- AD 3 :** Algorithm Definition, Accuracy and Specification - Bibli\_Alti : Altimeter Level 1b Processing  
**SALP-ST-M2-EA-15596-CN**
- AD 4 :** Algorithm Definition, Accuracy and Specification - Bibli\_Alti : Radiometer Level 1b Processing  
**SALP-ST-M2-EA-15597-CN**
- AD 5 :** Algorithm Definition, Accuracy and Specification - Bibli\_Alti : Altimeter Level 2 Processing  
**SALP-ST-M2-EA-15598-CN**
- AD 6 :** Algorithm Definition, Accuracy and Specification - Bibli\_Alti : Off-Line Control Processing  
**SALP-ST-M2-EA-15599-CN**
- AD 7 :** Algorithm Definition, Accuracy and Specification - Bibli\_Alti : Altimeter/Radiometer Verification Processing  
**SALP-ST-M2-EA-15703-CN**
- AD 8 :** Algorithm Definition, Accuracy and Specification - Bibli\_Alti : Mechanisms  
**SALP-ST-M2-EA-15600-CN**
- AD 9 :** SALP Products Specification - Volume 10 : Jason-2 User Products  
**SALP-ST-M-EA-15704-CN**
  
- RD 1 :** TOPEX/POSEIDON Project, 1992, "GDR-T User's Handbook"  
**PD 633-721, JPL D-8944, October 18, 1993**
- RD 2 :** AVISO and PODAAC User Handbook - IGDR and GDR Jason Products  
**SMM-MU-M5-OP-13184-CN (AVISO), JPL D-21352 (PODAAC)**
- RD 3 :** Rain Flag Modification for Version B Jason GDRs  
**Doc. Techni/ DOPS/LOS, 2006-01**



**Contents**

- 1. Introduction ..... 1**
  - 1.1. Overview of the OSTM/Jason-2 product family ..... 1**
    - 1.1.1. Product contents ..... 1
    - 1.1.2. Filename conventions ..... 2
  - 1.2. Handbook Overview ..... 4**
  - 1.3. Document reference and contributors ..... 4**
  - 1.4. Conventions..... 5**
    - 1.4.1. Vocabulary ..... 5**
      - 1.4.1.1. Altimetric distances .....5
      - 1.4.1.2. Orbits, Revolutions, Passes, and Repeat Cycles.....5
      - 1.4.1.3. Reference Ellipsoid .....6
    - 1.4.2. Correction Conventions ..... 6**
    - 1.4.3. Time Convention..... 6**
    - 1.4.4. Unit Convention..... 6**
    - 1.4.5. Flagging and Editing..... 6**
- 2. OSTM/Jason-2 Mission Overview ..... 7**
  - 2.1. Background ..... 7**
  - 2.2. OSTM/Jason-2 Mission ..... 7**
  - 2.3. OSTM/Jason-2 Requirements ..... 8**
    - 2.3.1. Accuracy of Sea-level Measurements ..... 8
    - 2.3.2. Sampling Strategy..... 9
    - 2.3.3. Tidal Aliases..... 9
    - 2.3.4. Duration and coverage ..... 9
  - 2.4. Satellite Description ..... 9**
    - 2.4.1. Satellite Characteristics..... 11**
    - 2.4.2. Sensors ..... 11**
      - 2.4.2.1. Poseidon-3 Altimeter..... 11
      - 2.4.2.2. Advanced Microwave Radiometer (AMR)..... 11
      - 2.4.2.3. DORIS System ..... 12
      - 2.4.2.4. Laser Reflector Array ..... 13
      - 2.4.2.5. GPS Receiver ..... 13
      - 2.4.2.6. CARMEN-2 Radiation Detectors..... 13
      - 2.4.2.7. LPT Detection Unit ..... 14
      - 2.4.2.8. T2L2 Detectors ..... 14
    - 2.4.3. Orbit ..... 14**
      - 2.4.3.1. Repetitive orbit on historical ground track (June 2008 - October 2016)..... 14



---

2.4.3.1.1. Equator Crossing Longitudes (in order of Pass Number) .....	17
2.4.3.1.2. Equator Crossing Longitudes (in order of Longitude) .....	18
2.4.3.2. Repetitive orbit on interleaved orbit (October 2016-July 2017) .....	19
2.4.3.2.1. Equator Crossing Longitudes (in order of Pass Number) .....	19
2.4.3.2.2. Equator Crossing Longitudes (in order of Longitude) .....	20
2.4.3.3. Repetitive orbit on Long Repeat orbit (July 2017-July 2018) .....	21
2.4.3.4. Repetitive orbit on Interleaved Long Repeat orbit (July 2018-nowadays).....	21
2.4.4. The OSTM/Jason-2 Project Phases .....	21
<b>2.5. Data Processing and Distribution .....</b>	<b>22</b>
2.5.1. Access to NRT data .....	23
2.5.2. Access to off-line data .....	23
2.5.3. Documentation and Sample Reader Software .....	23
<b>2.6. Access to data via NOAA.....</b>	<b>23</b>
2.6.1. Access to NRT data .....	23
2.6.2. Access to off line data .....	24
<b>2.7. Access to data via EUMETSAT .....</b>	<b>24</b>
2.7.1. NRT data access .....	24
2.7.2. Access to archived data .....	24
<b>2.8. Access to data on GTS .....</b>	<b>24</b>
2.8.1.1. GTS access for OGDR-BUFR files .....	24
<b>2.9. CNES data distribution .....</b>	<b>24</b>
2.9.1. Details of off line data access via CNES.....	24
<b>2.10. Jason-1 Data Products at AVISO and PODAAC .....</b>	<b>25</b>
2.10.1. Jason-1 Products on AVISO FTP Server. ....	25
2.10.2. Jason-1 Products on PODAAC FTP Server. ....	25
<b>3. Product evolution history.....</b>	<b>26</b>
<b>3.1. Models and Standards History .....</b>	<b>26</b>
3.1.1. GDR Product Version "T" and O/IGDR Product Version "c" .....	26
3.1.1.1. Models and Standards .....	26
3.1.1.2. Sea Surface Height Bias.....	27
3.1.1.3. Time-tag Bias .....	27
3.1.2. Version "d" Products .....	28
3.1.2.1. Models and Standards .....	28
3.1.2.2. Sea Surface Height Bias.....	29
<b>3.2. Models and Editing on Version "d" Products .....</b>	<b>31</b>
3.2.1. Orbit models .....	31
3.2.2. Mean Sea Surface .....	35
3.2.3. Mean Dynamic Topography .....	37



---

3.2.4. Geoid .....	37
3.2.5. Bathymetry.....	38
3.2.6. Ocean Tides .....	38
3.2.6.1. GOT4.8 Ocean Tide Model .....	39
3.2.6.2. FES2004 Ocean Tide Model.....	39
3.2.7. Data Editing Criteria .....	42
<b>4. Using the (O)(I)GDR data .....</b>	<b>43</b>
<b>4.1. Overview .....</b>	<b>43</b>
<b>4.2. Typical computation from altimetry data.....</b>	<b>44</b>
4.2.1. Corrected Altimeter Range .....	44
4.2.2. Sea Surface Height and Sea Level Anomaly.....	45
4.2.2.1. Tide Effects .....	46
4.2.2.2. Geophysical Surface - Mean Sea Surface or Geoid .....	47
4.2.3. Mean Sea Surface and Adjustment of the Cross Track Gradient .....	47
4.2.4. Smoothing Ionosphere Correction .....	48
4.2.5. Total Electron Content from Ionosphere Correction .....	48
4.2.6. Range Compression.....	48
<b>5. Altimetric data .....</b>	<b>50</b>
5.1. Precise Orbits .....	50
5.2. Altimeter Range.....	50
5.3. Geoid.....	50
5.4. Mean Sea Surface .....	50
5.5. Mean Dynamic Topography .....	51
5.6. Geophysical Corrections.....	51
5.6.1. Troposphere (dry and wet).....	51
5.6.2. Ionosphere .....	52
5.6.3. Ocean Waves (sea state bias) .....	53
5.7. Rain Flag.....	53
5.8. Ice Flag .....	54
5.9. Tides .....	55
5.9.1. Geocentric Ocean Tide .....	56
5.9.2. Long period Ocean Tide .....	56
5.9.3. Solid Earth Tide .....	57
5.9.4. Pole Tide.....	57
5.10. Inverse Barometer Effect.....	58
5.10.1. Inverted Barometer Correction .....	58
5.10.2. Barotropic/Baroclinic Response to Atmospheric Forcing .....	58



---

5.11. Sigma 0 .....	59
5.12. Wind Speed .....	59
5.13. Bathymetry Information .....	59
<b>6. Data description .....</b>	<b>60</b>
<b>6.1. Data format .....</b>	<b>60</b>
6.1.1. NetCdf format and CF convention .....	61
6.1.2. The NetCDF Data Model .....	61
6.1.2.1. Dimensions .....	61
6.1.2.2. Variables .....	61
6.1.2.3. Coordinate variables and auxiliary coordinate variables .....	61
6.1.2.4. Attributes .....	61
6.1.3. The Common Data Language .....	61
<b>6.2. Global attributes .....</b>	<b>61</b>
<b>6.3. Data Sets .....</b>	<b>61</b>
<b>6.4. Software .....</b>	<b>61</b>
6.4.1. Software provided with netCDF : “ncdump” .....	61
6.4.2. Additional general software .....	61
6.4.2.1. ncbrowse .....	61
6.4.2.2. netCDF Operator (NCO) .....	61
6.4.3. Additional specific software : “BRAT” .....	61
<b>6.5. OGDR BUFR product .....</b>	<b>62</b>
<b>Annexe A - References .....</b>	<b>63</b>
<b>Annexe B - List of acronyms .....</b>	<b>66</b>
<b>Annexe C - Contacts .....</b>	<b>68</b>



## 1. Introduction

OSTM/Jason-2 is a follow-on mission to Jason-1. The satellite is named after the leader of the Argonauts' famous quest to recover the Golden Fleece. The OSTM/Jason-2 mission takes over and continues the TOPEX/Poseidon and Jason-1 missions. While the TOPEX/Poseidon and Jason-1 missions were conducted under a cooperation between the French Space Agency, "Centre National d'Etudes Spatiales" (CNES) and the United States National Aeronautics and Space Administration (NASA), OSTM/Jason-2 involves CNES, NASA and 2 new partners : the European Organisation for the Exploitation of Meteorological Satellites (EUMETSAT) and the National Oceanic and Atmospheric Administration (NOAA) in order to facilitate the transition towards a fully operational altimetry mission, able to satisfy the data timeliness and reliability requirements of operational applications.

### 1.1. Overview of the OSTM/Jason-2 product family

The purpose of this document is to assist users of the OSTM/Jason-2 products (Operational Geophysical Data Record : OGDR, Interim Geophysical Data Record : IGDR, and Geophysical Data Record : GDR) by providing a comprehensive description of product content and format. We will so refer to (O)(I)GDR in this document when the information is relevant for all the products.

(O)(I)GDR products are identical except for the following differences regarding the auxiliary data used in the processing:

Auxiliary Data	Impacted Parameter	OGDR	IGDR	GDR
Orbit	Satellite altitude, Doppler correction, ...	DORIS Navigator	Preliminary (MOE using DORIS data and/or GPS data*)	Precise (POE using DORIS and/or GPS data)
Meteo Fields	Dry/wet tropospheric corrections, U/V wind vector, Surface pressure, Inverted barometer correction, ...	Predicted	Restituted	
Pole Location	Pole tide height	Predicted		Restituted
Mog2D	HF ocean dealiasing correction	Not available	Preliminary	Precise
GIM	Ionosphere correction	Not available	Available	
Radiometer antenna temperatures coeff.	Wet tropospheric correction, Sigma0 rain attenuation, ...	Preliminary		Precise (accounting for radiometer calibration)

Table 1. Differences between Auxiliary Data for O/I/GDR Products

GDR products, unlike OGDR and IGDR products, are fully validated products.

\* MOE uses only DORIS data before February 12<sup>th</sup>, 2019 and DORIS+GPS data afterwards

Please note that contrary to previous standard, OGDR and IGDR are not available for "F" standard which is a No Time Critical standard only.

#### 1.1.1. Product contents

The Level-2 products from this mission comprise a family of nine different types of geophysical data records (GDRs). As illustrated in Table 1 below, there are three families of GDRs, distinguished by increasing latency and accuracy, going from the Operational GDR (OGDR), to the Interim GDR (IGDR),



to the final GDR. Within each of these three families there are up to three types of files in NetCDF format, with increasing size and complexity:

1. a reduced 1 Hz subset of the full dataset in NetCDF format (O/I/GDR-SSHA);
2. the native NetCDF formatted datasets (O/I/GDRs) which contain 1Hz records as well as 20 Hz high-rate values;
3. an expert sensor product containing the full radar-echo waveforms in NetCDF format (S-IGDR/S-GDR, not applicable to the OGDR).

For the OGDR family, a specific product in BUFR format containing exclusively 1 Hz data is available, designed to cover the needs of the operational community for near real time observations in World Meteorological Organisation (WMO) standardised formats for assimilation in Numerical Weather Prediction (NWP) models.

**OSTM/Jason-2 Level-2 Products**

	OGDR family	IGDR family	GDR family	<b>Size &amp; Complexity</b> 
<b>Reduced 1Hz</b>	OGDR-SSHA	IGDR-SSHA	GDR-SSHA	
<b>1Hz + 20Hz</b>	OGDR OGDR-BUFR*	IGDR	GDR	
<b>1Hz + 20Hz +waveforms</b>	-	S-IGDR	S-GDR	
<b>Latency</b>	3 - 5 Hours	1 day	~ 90 days	



\*All files in NetCDF format except OGDR-BUFR, which contains no 20Hz data

**Table 2.** Summary of operational, interim, and final geophysical data record products (O/I/GDR) from the Jason-2 / Ocean Surface Topography Mission (OSTM).

All nine files contain sea surface height, ocean surface wind speed, significant wave height information and all required corrections. The NetCDF files differ in the amount and type of auxiliary data included but the product format is the same.

**1.1.2. Filename conventions**

The product names are based on the following convention:

JA2\_<O/I/G>P<N/R/S>\_2P<v><S/P><ccc>\_<ppp>\_<yyyymmdd\_hhnnss>\_<yyyymmdd\_hhnnss>.nc

With :

- <O/I/G> : product family (O : OGDR, I : IGDR, G: GDR)
- <N/R/S> : product type (N : native, R: reduced, S : sensor)
- <v> : product version (set to 'T' during CalVal phases, set to 'c', the current Jason-1 data standards, for the first delivery of OSTM/Jason-2 products to users, set to 'd' for the reprocessed delivery)
- <S/P> : product duration (S : segment for OGDR, P : pass for I/GDR)



<ccc>: cycle number of 1<sup>st</sup> product record  
<ppp> : pass number of 1<sup>st</sup> product record (1-254)  
<yyyymmdd\_hhnnss> : date of 1<sup>st</sup> product record  
<yyyymmdd\_hhnnss> : date of last product record

So for the OGDR we have:

OGDR: JA2\_OPN\_2PvSccc\_ppp\_yyyyymmdd\_hhnnss\_yyyyymmdd\_hhnnss.nc  
OGDR-SSHA: JA2\_OPR\_2PvSccc\_ppp\_yyyyymmdd\_hhnnss\_yyyyymmdd\_hhnnss.nc

for the OGDR-BUFR, the filename is not relevant if your are accessing the files via GTS (see below for details on access to NRT data). Otherwise, if you are accessing the files from the archives (CLASS or UMARF) or EUMETCast, the filenames of the OGDR-BUFR are:

at the NOAA/CLASS:

JA2\_OPB\_2PvSccc\_ppp\_yyyyymmdd\_hhnnss\_yyyyymmdd\_hhnnss

at the EUMETSAT/UMARF and on EUMETCast:

W\_US-NOAA-

Washington,SURFACE+SATELLITE,JASON2+OGDR\_C\_KNES\_yyyyymmddhhnnss\_v\_ccc\_ppp\_yyyyymmddhhnnss.bin

W\_XX-EUMETSAT-

Darmstadt,SURFACE+SATELLITE,JASON2+OGDR\_C\_EUMS\_yyyyymmddhhnnss\_v\_ccc\_ppp\_yyyyymmddhhnnss.bin

for the IGDR:

IGDR: JA2\_IPN\_2PvPccc\_ppp\_yyyyymmdd\_hhnnss\_yyyyymmdd\_hhnnss.nc  
IGDR-SSHA: JA2\_IPR\_2PvPccc\_ppp\_yyyyymmdd\_hhnnss\_yyyyymmdd\_hhnnss.nc  
S-IGDR: JA2\_IPS\_2PvPccc\_ppp\_yyyyymmdd\_hhnnss\_yyyyymmdd\_hhnnss.nc

and for the GDR:

GDR: JA2\_GPN\_2PvPccc\_ppp\_yyyyymmdd\_hhnnss\_yyyyymmdd\_hhnnss.nc  
GDR-SSHA: JA2\_GPR\_2PvPccc\_ppp\_yyyyymmdd\_hhnnss\_yyyyymmdd\_hhnnss.nc  
S-GDR: JA2\_GPS\_2PvPccc\_ppp\_yyyyymmdd\_hhnnss\_yyyyymmdd\_hhnnss.nc



---

## 1.2. Handbook Overview

---

This is a combination of a guide to data use and a reference handbook, so not all sections will be needed by all readers.

**Section 1** provides information on product evolution history

**Section 2** provides background information about the (O)(I)GDR and this document

**Section 3** is an overview of the OSTM/Jason-2 mission

**Section 4** is an introduction to using the OSTM/Jason-2 data

**Section 5** is an introduction to the OSTM/Jason-2 altimeter algorithms

**Section 6** provides a description of the content and format of the OSTM/Jason-2 (O)(I)GDRs

**Appendix A** contains references

**Appendix B** contains acronyms

**Appendix C** describes how to order information or data from CNES, EUMETSAT and NOAA, and lists related Web sites.

---

## 1.3. Document reference and contributors

---

When referencing this document, please use the following citation:

“OSTM/Jason-2 Products Handbook”,

<b>CNES :</b>	<b>SALP-MU-M-OP-15815-CN</b>
<b>EUMETSAT :</b>	<b>EUM/OPS-JAS/MAN/08/0041</b>
<b>JPL :</b>	<b>OSTM-29-1237</b>
<b>NOAA/NESDIS :</b>	<b>Polar Series/OSTM J400</b>

Other contributors include:

J.P. Dumont, L. Carrère and V. Rosmorduc from CLS

Remko Scharroo from EUMETSAT

S. Desai from NASA/JPL

H. Bonekamp and J. Figa from EUMETSAT

E. Bronner, A. Couhert and N. Picot from CNES

## 1.4. Conventions

### 1.4.1. Vocabulary

#### 1.4.1.1. Altimetric distances

In order to reduce confusion in discussing altimeter measurements and corrections, the following terms are used in this document as defined below:

- **Distance** and **Length** are general terms with no special meaning in this document
- **Range** is the distance from the satellite to the surface of the Earth, as measured by the altimeter. Thus, the altimeter measurement is referred to as "range" or "altimeter range," not height
- **Altitude** is the distance of the satellite or altimeter above a reference point. The reference point used is the reference ellipsoid. This distance is computed from the satellite ephemeris data
- **Height** is the distance of the sea surface above the reference ellipsoid. The sea surface height is the difference of the altimeter range from the satellite altitude above the reference ellipsoid

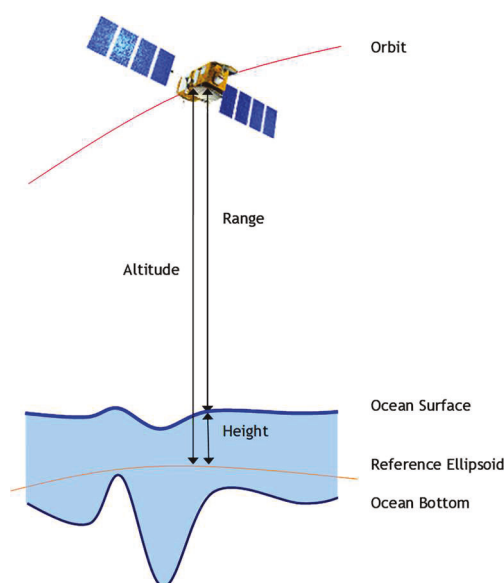


Figure 1 : Altimetric distances - Altitude, Range and Height

#### 1.4.1.2. Orbits, Revolutions, Passes, and Repeat Cycles

An **Orbit** is one circuit of the earth by the satellite as measured from one ascending node crossing to the next. An ascending node occurs when the sub satellite point crosses the earth's equator going from south to north. A **Revolution** (REV) is synonymous with orbit.



The OGDR data is organized into files (“segments”) which corresponds to the amount of data dumped over an Earth terminal (typically 2 hour-data sets).

The (I)GDR data is organized into pass files in order to avoid having data boundaries in the middle of the oceans, as would happen if the data were organized by orbit. A **Pass** is half a revolution of the earth by the satellite from extreme latitude to the opposite extreme latitude.

For OSTM/Jason-2, an **Ascending Pass** begins at the latitude -66.15 deg and ends at +66.15 deg. A **Descending Pass** is the opposite (+66.15 deg to -66.15 deg). The passes are numbered from 1 to 254 representing a full repeat cycle of the OSTM/Jason-2 ground track. Ascending passes are odd numbered and descending passes are even numbered.

After one **repeat cycle** of 254 passes, OSTM/Jason-2 revisits the same ground-track within a margin of  $\pm 1$  km. That means that every location along the OSTM/Jason-2 ground-track is measured every approximately 9.9 days.

After July 10<sup>th</sup> of 2017 Jason-2 was transferred to a “Long Repeat Orbit” (LRO) at 1309km altitude. The ground track is no longer repeatable on 9.9 days; its actual cycle is now 368 days composed of 4736 revolutions. In order to discriminate products before and after orbit lowering, cycles are restarted from number 500 on 2017/07/10 at 04:43:08. However, the conventions remain the same: products are still referenced to 10-day cycles of 254 passes.

After July 13<sup>th</sup> of 2018, Jason-2 was transferred to the “interleaved LRO”: its ground track is translated of 4km in order to increase the precision of measurement on the geoid. Cycles are restarted from number 600 on 2018/07/18 at 13:20:12.

### 1.4.1.3. Reference Ellipsoid

The **Reference Ellipsoid** is the first-order definition of the non-spherical shape of the Earth as an ellipsoid of revolution.

Historically, the reference ellipsoid had an equatorial radius of 6378.1363 kilometers and a flattening coefficient of 1/298.257 (same reference ellipsoid as historically used by the Jason-1 and the T/P missions).

Since GDR-F Standard, the **Reference Ellipsoid** has an equatorial radius of 6378.1370 kilometers and a flattening coefficient of 1/298.257223563 (WGS84 ellipsoid).

### 1.4.2. Correction Conventions

All environmental and instrument corrections are computed so that they should be added to the quantity which they correct. That is, a correction is applied to a measured value by

$$\text{Corrected Quantity} = \text{Measured Value} + \text{Correction}$$

This means that a correction to the altimeter range for an effect that lengthens the apparent signal path (e.g., wet troposphere correction) is computed as a negative number. Adding this negative number to the uncorrected (measured) range reduces the range from its original value toward the correct value. Example: Corrected Range = Measured Range + Range Correction.

### 1.4.3. Time Convention

Times are UTC and referenced to **January 1, 2000 00:00:00.00**.

A UTC leap second can occur on June 30 or December 31 of any year. The leap second is a sixty-first second introduced in the last minute of the day. Thus the UTC values (minutes:seconds) appear as: 59:58 ; 59:59 ; 59:60 ; 00:00 ; 00:01.

### 1.4.4. Unit Convention

All distances and distance corrections are reported in tenths of millimeters ( $10^{-1}$  mm).

### 1.4.5. Flagging and Editing

In general, flagging consists of three parts: instrument flags (on/off), telemetry flags (preliminary flagging and editing) and data quality flags (geophysical processing flags).

Instrument flags provide information about the state of the various instruments on the satellite.



Telemetry flags are first based on instrument modes and checking of telemetry data quality. Only severely corrupted data are not processed (i.e. data that cannot be correctly read on ground). Flag setting is designed to get a maximum amount of data into the “Sensor Data Records” (part of the SGDR data sets). Science data are processed only when the altimeter is in tracking mode.

Quality flags are determined from various statistical checks on the residuals after smoothing or fitting through the data themselves. These flags are set if gaps in the data are detected, or residuals have exceeded predetermined thresholds, or if the gradients of the data exceed predetermined thresholds.

## 2. OSTM/Jason-2 Mission Overview

### 2.1. Background

Two previous high-accuracy altimetric missions, TOPEX/POSEIDON (T/P, launched in August 1992 and which last until October 2005) and Jason-1 (launched in December 2001) have been the key elements of a major turning point in physical oceanography, in terms of both scientific research and applications. Exceeding most initial specifications in terms of accuracy, T/P quickly became a unique tool to make significant progress in the understanding and modeling of ocean circulation and consequently on its climatic impact. The success of the T/P mission was mainly due to an appropriate optimization of the system: instruments, satellite, and orbit parameters were all specifically designed to fulfill the objectives of the mission. The T/P follow-on mission, Jason-1, was engaged soon after with the aim to provide the same level of performance, but with a significant decrease in weight and power needs, hence a much lower mission cost. In addition, near-real time applications were included in the main objectives of the mission.

Both missions, individually as well as combined have made essential contributions in other domains, like mean sea level surveys, tides, marine meteorology, geophysics and geodesy. Most notably the tandem mission phase, where Jason-1 and T/P were flying on the same orbit separated by only 70 s, provided a unique opportunity for intercalibration of both systems, hence improving further the scientific data quality. High accuracy radar altimeter missions are uniquely capable to globally and continuously observe the ocean and to better understand the short to long term changes of ocean circulation. They are now considered as essential components of global ocean observation systems. These systems integrate altimetric and other satellite and in-situ data into models and require the continuity and permanence of ocean measurements to produce time series over several decades.

The near-real time and short term capability of Jason-1 as well as ENVISAT (from ESA, launched in March 2002) have fed several pilot experiments that demonstrated the growing importance of operational ocean observation products and short-range ocean prediction for a variety of applications (ship routing, environmental hazards, support to maritime industries).

Also worth mentioning is the importance of wave and wind data provided by altimeter systems over oceans. This information is routinely used in meteorological and research entities, either for calibration of other data sets, assimilation in weather and wave models, or for statistical analysis.

### 2.2. OSTM/Jason-2 Mission

The OSTM/Jason-2 mission is built on the heritage of T/P and Jason-1, with two driving ambitions:

- Ensuring continuity of high quality measurements for ocean science
- Providing operational products for assimilation and forecasting applications

The main participation of the agencies is the following:

- CNES has provided the platform and payload module (see section 2.4)
- NASA and CNES have jointly provided the payload instruments (see section 2.4)
- NASA has provided launch services for the satellite



- CNES provides a command and control center for the satellite, a European Earth Terminal and data processing, archiving and distribution infrastructure for the mission
- NOAA provides a control center for the satellite, command and data acquisition (CDA) stations and data processing, archiving and distribution infrastructure for the mission
- EUMETSAT provides a site and infrastructure for accommodation of the European Earth terminal, to be integrated into the EUMETSAT Ground Segment infrastructure and data processing, archiving and near real time products distribution infrastructure for the mission

OSTM/Jason-2 was launched on **20 June 2008 at 7:46 GMT** and reached its **nominal repetitive orbit** on 4 July 2008. The start of cycle 1 occurred on 12 July 2008 at 01:20:05 GMT.

OSTM/Jason-2 was moved from nominal ground track early October 2016. After a series of maneuvers, the satellite reached the **interleaved orbit on October 14<sup>th</sup> 2016** in the middle of cycle 305.

OSTM/Jason-2 was moved from the interleaved orbit ground track to the Long Repeat Orbit (27km below the nominal orbit), and restarted measurements on LRO on July 10<sup>th</sup>, 2017.

OSTM/Jason-2 was moved from the Long Repeat Orbit to the Interleaved Long Repeat Orbit (I-LRO), and restarted measurements on July 18<sup>th</sup>, 2018.

OSTM/Jason-2 was removed from service on October 1<sup>st</sup>, 2019, after more than 11 years of service.

The Jason missions support research programs such as the Climate Variability and Predictability program (CLIVAR) and the Global Ocean Data Assimilation Experiment (GODAE).

## 2.3. OSTM/Jason-2 Requirements

---

The major elements of the mission include:

- **An Earth orbiting satellite carrying an altimetric system** for measuring the height of the satellite above the sea surface
- **A precision orbit determination system** for referring the altimetric measurements to geodetic coordinates
- **A data analysis and distribution system** for processing the satellite data, verifying their accuracy, and making them available to the scientific community
- **A Principal Investigator program** for feedback from operational applications and scientific studies based on the satellite observations

The sea-surface height measurement must be made with an accuracy of 3.4 cm or better (at 1 Hz) in order to meet the mission objectives. The OSTM/Jason-2 satellite is specified and designed to fulfill the mission objectives (AD 1) and to take over from the Jason-1 mission. As for Jason-1, distribution of altimetric products (non-validated) in near real time is planned. The interim (IGDR) and definitive (GDR) science products are delivered later (see Table 21 in section 6), following the model used for Jason-1.

To ensure that science and mission goals are accomplished by the OSTM/Jason-2 mission, the following requirements were established.

### 2.3.1. Accuracy of Sea-level Measurements

Generally speaking OSTM/Jason-2 has been specified based on the Jason-1 state of the art, including improvements in payload technology, data processing and algorithms or ancillary data (e.g: precise orbit determination and meteorological model accuracy). The sea-surface height shall be provided with a globally averaged RMS accuracy of 3.4 cm (1 sigma), or better, assuming 1 second averages.

The instrumental and environmental corrections are provided with the appropriate accuracy to meet this requirement. In addition to these requirements, a set of measurement-system goals was established based on the anticipated impact of off-line ground processing improvements. These improvements are expected to enable reduction of sea-surface height errors to 2.5 cm RMS. Knowledge of the stability of the system is especially important to the goal of monitoring the change



in the global mean sea level, hence a specification on the system drift with a 1 mm/year goal. The following table provides a summary of specifications and error budget at the end of the verification phase.

Parameter	OGDR 3 hours		IGDR 1 to 1.5 days		GDR 40 days		
	Requirement	Actual	Requirement	Actual	Requirement	Goal	Actual
Altimeter Noise <sup>1</sup>	1.7	1.8	1.7	1.8	1.7	1.5	1.8
Ionosphere <sup>2</sup>	1	0.3	0.5	0.3	0.5	0.5	0.3
Sea State Bias <sup>3</sup>	3.5	2	2	2	2	1	2
Dry Troposphere	1	0.8	0.7	0.7	0.7	0.7	0.7
Wet Troposphere	1.2	0.8	1.2	0.8	1.2	1	0.8
<b>Altimeter Range, RSS</b>	<b>5</b>	<b>2.9</b>	<b>3</b>	<b>2.9</b>	<b>3</b>	<b>2.25</b>	<b>2.9</b>
RMS Orbit (Radial Component)	10 <sup>(4)</sup>	3.0 <sup>(4)</sup>	2.5	1.5	1.5	1.0	1.0
<b>Total Sea Surface Height, RSS</b>	<b>11.2</b>	<b>4.2</b>	<b>3.9</b>	<b>3.3</b>	<b>3.4</b>	<b>2.5</b>	<b>3.1</b>
Significant Wave Height <sup>5</sup>	10% or 0.5 m	TBD % or 0.12 m	10% or 0.4m	TBD % or 0.12 m	10% or 0.4m	5% or 0.25m	TBD % or 0.12 m
Wind Speed	1.6 m/s	0.9 m/s	1.5 m/s	0.9 m/s	1.5 m/s	1.5 m/s	0.9 m/s
Sigma Naught (absolute)	0.7 dB	0.1 <sup>(6)</sup> dB	0.7 dB	0.1 <sup>(6)</sup> dB	0.7 dB	0.5 dB	0.1 <sup>(6)</sup> dB
System Drift						1 mm/year <sup>(7)</sup>	TBD

(1) – Ku-Band after ground retracking, averaged over 1 second, assuming 320 MHz C-Band bandwidth.  
 (2) – Filtered over 100 km assuming 320 MHz bandwidth.  
 (3) – Can also be expressed as 1% of SWH.  
 (4) – Real-time DORIS onboard ephemeris.  
 (5) – Whichever is greater.  
 (6) – After calibration to Jason-1.  
 (7) – On global mean sea level, after calibration.

Table 3 : Summary of error budget at the end of the verification phase

### 2.3.2. Sampling Strategy

As for Jason-1, sea level shall be measured along a fixed grid of subsatellite tracks such that it is possible to investigate and minimize the spatial and temporal aliases of surface geostrophic currents and to minimize the influence of the geoid on measurements of the time-varying topography.

### 2.3.3. Tidal Aliases

As for Jason-1, sea level shall be measured such that tidal signals are not aliased into semiannual, annual, or zero frequencies (which influences the calculation of the permanent circulation) or frequencies close to these.

### 2.3.4. Duration and coverage

Sea level shall be measured for a minimum of five years, with the potential to extend this period for an additional two years.

The OSTM/Jason-2 satellite shall overfly the reference Jason-1 ground tracks.

## 2.4. Satellite Description

The 500 kg satellite consists of a multi-mission PROTEUS platform and an OSTM/Jason-2 specific payload module. Both are provided by CNES. The platform provides all housekeeping functions including propulsion, electrical power, command and data handling, telecommunications, and attitude control. The payload module provides mechanical, electrical, thermal, and dynamical support to the OSTM/Jason-2 instruments.

The OSTM/Jason-2 payload (see Figure 2) includes the following components:

- **An Altimeter (Poseidon-3)**, provided by CNES - the main mission instrument
- **A Microwave Radiometer (AMR)**, provided by NASA - to correct the altimeter measurement for atmospheric range delays induced by water vapor
- **The radio positioning DORIS system**, provided by CNES - for precision orbit determination using dedicated ground stations
- **A Laser Reflector Array**, provided by NASA - to calibrate the orbit determination system
- **A precision GPS receiver (GPSP)**, provided by NASA - to provide supplementary positioning data to DORIS in support of the POD function and to enhance and/or improve gravity field models
- Three experimental passengers:
  - **CARMEN-2 Radiation Detectors**, provided by CNES - to measure high-energy particles that could disturb the ultra-stable oscillator in the DORIS positioning unit
  - **A Light Particle Telescope (LPT) detection unit**, provided by JAXA under CNES responsibility - complementing the measurement of radiation received by the DORIS instrument
  - **Time Transfer by Laser Link (T2L2) detectors**, provided by CNES - for ultra-precise time transfer, to monitor the clock in the DORIS instrument

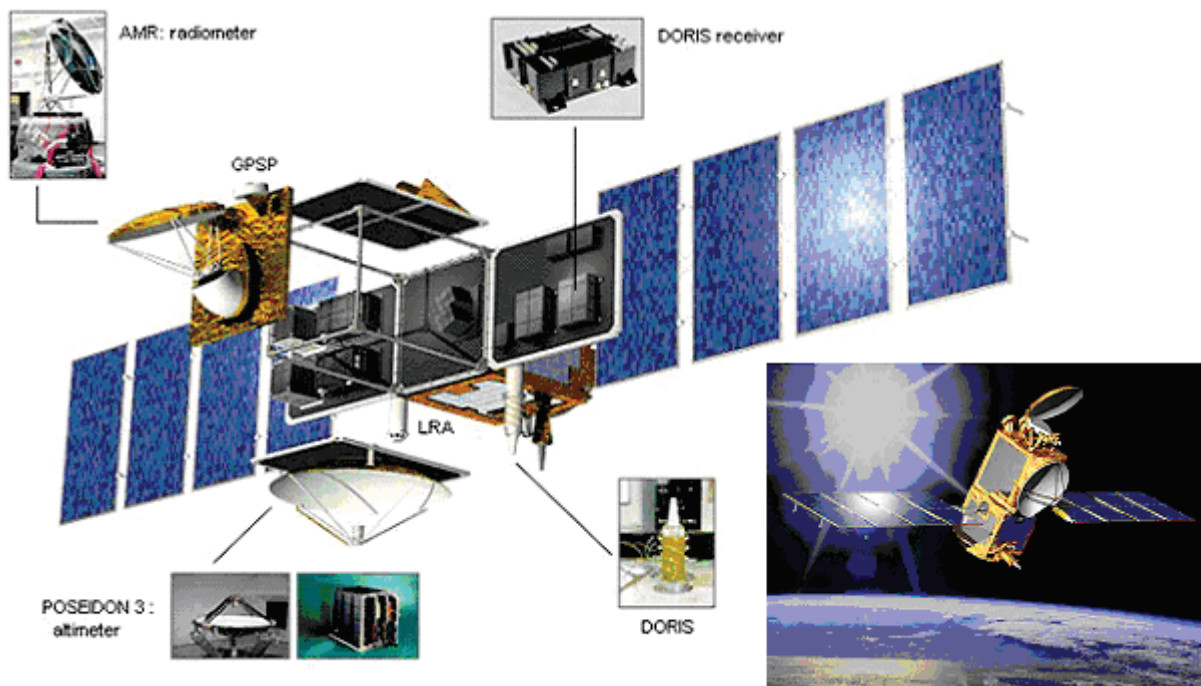


Figure 2 : OSTM/Jason-2 satellite (main components and artist view)

## 2.4.1. Satellite Characteristics

The main features of the OSTM/Jason-2 satellite are summed up in the following table.

Satellite mass	525 kg
Satellite power	511 W
Platform mass	270 kg
Platform power	300 W
Payload mass	120 kg
Payload power	147 W
Altimeter mass	55 kg
Altimeter power	78 W
Launch Vehicle	Delta II (7320)
Launch Site	Vandenberg Air Force Base (AFB)

**Table 4** : Main features of the OSTM/Jason-2 satellite

## 2.4.2. Sensors

### 2.4.2.1. Poseidon-3 Altimeter

The two-frequency solid-state altimeter, measuring range with accurate ionospheric corrections, is derived from the two-frequency Poseidon-2 altimeter embarked on Jason-1 mission and from the SIRAL altimeter. It operates at 13.575 GHz (Ku-band) and 5.3 GHz (C-band). Poseidon-3 electronics are configured in two boxes: the processing unit (PCU) and the radiofrequency unit (RFU).

- The processing unit includes the digital chirp generator, base-band demodulator, spectrum analyzer, instrument control unit and interfaces.
- The RF unit includes the up-conversion to the Ku and C bands, high power amplifier (solid state), low noise amplification of the received echoes and mixing with a reference chirp. The peak output powers are 6 to 8 W for the Ku band and 25 W for the C band.
- Poseidon-3 is dual string (in cold redundancy) without cross strapping and connected to the antenna through a switching box.
- Poseidon-3 antenna is of centered type (1.2 meter diameter) and located on the nadir face of the satellite.



**Figure 3** : OSTM/Jason-2 Posidon-3 Instrument

### 2.4.2.2. Advanced Microwave Radiometer (AMR)

The three frequency microwave radiometer, named the Advanced Microwave Radiometer, consists of three separate channels at 18.7, 23.8 and 34 GHz. The radiometer is functionally equivalent to the Jason Microwave Radiometer found on Jason-1. The 23.8 GHz channel is the primary water vapor sensing channel, meaning higher water vapor concentrations leads to larger 23.8 GHz brightness temperature values. The addition of the 34 GHz channel and the 18.7 GHz channel, which have less sensitivity to water vapor, facilitate the removal of the contributions from cloud liquid water and

excess surface emissivity of the ocean surface due to wind, which also act to increase the 23.8 GHz brightness temperature.

The AMR design is based on Monolithic Millimeter-wave Integrated Circuit (MMIC) technology and represents a giant leap forward from its predecessors (TMR and JMR) in both mass and size. Three redundant temperature controlled noise diodes are used for operational gain calibration in all the radiometers channels. The use of noise diodes eliminates the need for a cold sky calibration horn, which was employed on TMR. The JMR was the first space-borne radiometer to use noise diodes for calibration and the AMR is the second.

Another significant improvement in the AMR design is the addition of a 1-m reflector, compared to a 0.6 m reflector for TMR and JMR, which nearly doubles the spatial resolution of the AMR. The AMR is expected to produce reliable path delay measurements to within 15-20 km from the coast. The antenna is a fixed offset paraboloid (1 meter diameter) fed by a single three frequency coaxial corrugated horn feed. It is located on the front of the satellite (+ X axis) and its beam is co-aligned with the altimeter footprint.

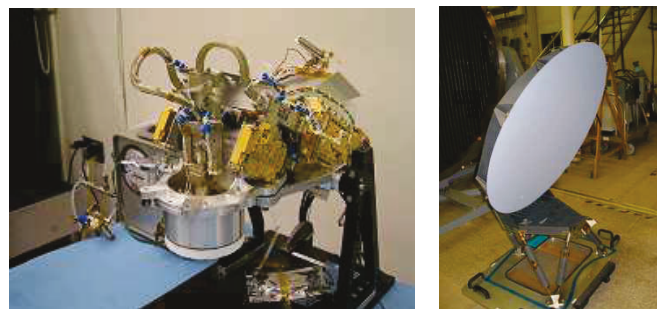


Figure 4 : OSTM/Jason-2 AMR Instrument and Antenna

### 2.4.2.3. DORIS System

The complete DORIS system includes the DORIS on board package, a network of approximately 50 beacons located around the world and a ground system.

The on board package includes the receiver itself, the ultrastable oscillator and an omnidirectional antenna located on the nadir face of the satellite.

The DORIS on board package is a new version of the DORIS instrument (all the functions included in a single unit). It includes a 8-beacons receiving capability and an on-board real time function (DIODE = “Détermination Immédiate d’Orbite par DORIS Embarqué”) to compute the orbit ephemeris.

The DORIS on board package is also dual string (in cold redundancy) without cross strapping and connected to the single antenna through a switching box. Each receiver is connected to its own ultra stable oscillator.

The DORIS antenna is located on the nadir side of the satellite.



Figure 5 : OSTM/Jason-2 DORIS Receiver Antenna and Instrument

## 2.4.2.4. Laser Reflector Array

The laser reflector array is placed on the nadir face of the satellite. It consists of several quartz corner cubes arrayed as a truncated cone with one in the center and the others distributed azimuthally around the cone.



Figure 6 : OSTM/Jason-2 Laser Reflector Array

## 2.4.2.5. GPS Receiver

The GPS Payload receiver is a twelve channel Global Positioning system receiver. The on board package is comprised of a down-converter processor assembly, two antennas and interconnecting RF cables.

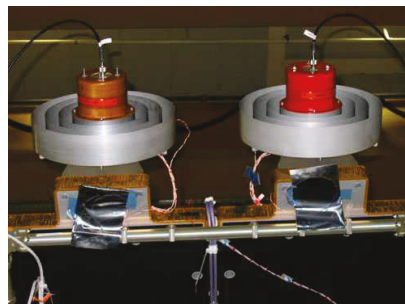


Figure 7 : OSTM/Jason-2 Precision GPS Receiver

## 2.4.2.6. CARMEN-2 Radiation Detectors

CARMEN-2 is the mission name for the ICARE-NG instrument aboard OSTM/Jason-2 satellite.

This instrument is dedicated to study the influence of space radiation on advanced components to measure  $e^-$ ,  $p^+$  and ion fluxes in the energy ranges responsible for component effects (as ionizing dose, single event effect and displacement damage), to measure associated effects on test components, to characterize the local radiation environment for DORIS USO and to evaluate its potential drifts inside the SAA.

The on board package includes only ICARE-NG box that is composed of a CPU, data processing & TM/TC unit, a custom DC/DC converter, a Data acquisition unit for the set of three radiation detectors and the component test bed.



Figure 8 : OSTM/Jason-2 CARMEN-2 Instrument

### 2.4.2.7. LPT Detection Unit

The LPT Detection Unit is composed of one detector box (LPT) and one electronic box (LPT-E). All the electrical interfaces with the satellite are through the LPT-E.

The detectors are placed on the satellite in order to see the same radiation environment and at the vicinity of DORIS BDR. The LPT-S is an assembly of four sensors, each adapted to different particles and energy band.

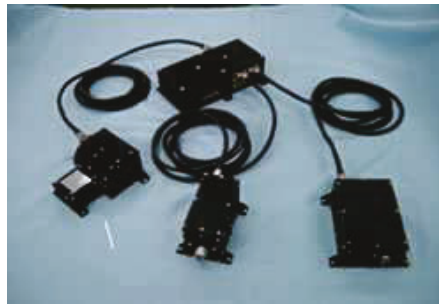


Figure 9 : OSTM/Jason-2 LPT

### 2.4.2.8. T2L2 Detectors

The T2L2 experiment onboard equipment is constituted of a photo-detection device, a time tagging unit and uses the Laser Reflector Array (LRA). The laser station emits light pulses in the OSTM/Jason-2 direction. The LRA returns a fraction of the received photons to the station.

The T2L2 onboard instrument is organized in 2 main subsystems: the optical one and the electronic one.

Two Optical Units collect a part of the laser pulse, one for the time dating and the other one for detection and amplitude measurement of the pulse.

The Electronic Unit ensures the conversion of the laser pulse into an electronic signal which is dated with a very high precision and the management of the whole instrument.



Figure 10 : OSTM/Jason-2 T2L2 Optics Unit

### 2.4.3. Orbit

#### 2.4.3.1. Repetitive orbit on historical ground track (June 2008 - October 2016)

The OSTM/Jason-2 satellite flies on the same ground-track as Jason-1 and the original T/P with a 254 pass, 10-day exact repeat cycle. As during the Jason-1 Cal/Val phase, Jason-2 was placed close to Jason-1 (1 minute apart) in order to allow inter-calibration of all systems. Then Jason-1 was moved to an interleaved ground track (as was T/P in August 2002).

Orbital characteristics and the equator crossing longitudes for OSTM/Jason-2 are given in Tables 10 and 11. Figure below is a plot of the ground track on a world map.

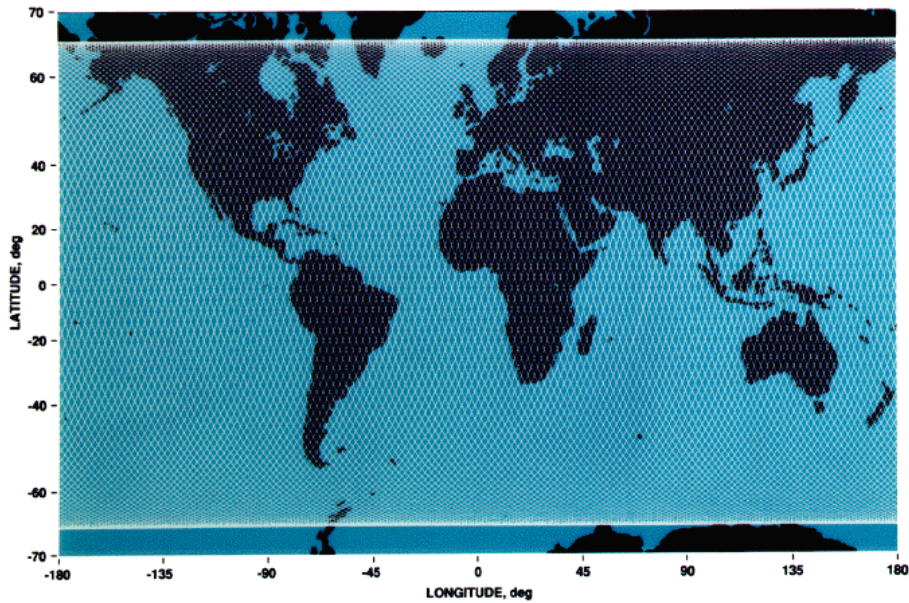


Figure 11 : T/P, Jason-1 and OSTM/Jason-2 ground track coverage every 10 days

The mean classical orbit elements are given in the table below.

Orbit element	Value
Semi-major axis	7,714.432 km
Eccentricity	0.000098
Inclination	66.042 deg
Argument of periapsis	90.0 deg
Inertial longitude of the ascending node	116.56 deg
Mean anomaly	253.13 deg

Table 5. Mean classical orbit elements

The orbit auxiliary data are given in the table below.

Auxiliary Data	Values
Reference (Equatorial) altitude	1,339 km
Nodal period	6,745.7605 sec
Repeat period	9.9156 days
Number of revolutions within a cycle	127
Equatorial cross-track separation	315 km
Ground track control band	± 1 km (at equator)
Acute angle at Equator crossings	39.4 deg
Longitude of Equator crossing of pass 1	99.9242 deg
Inertial nodal rate	- 2.07707 deg/day
Orbital speed	7.2 km/s
Ground track speed	5.8 km/s

Table 6 : Orbit auxiliary data

This orbit overflies two verification sites funded by NASA and CNES. The prime CNES verification site is located at Cape Senetosa on the island of Corsica (8°48' E, 41°34' N, ascending pass 85). The prime NASA verification site is located on the Harvest oil platform near Pt. Conception, California (239° 19' E, 34° 28' N, ascending pass 43).



---

A satellite orbit slowly decays due to air drag, and has long-period variability because of the inhomogeneous gravity field of Earth, solar radiation pressure, and smaller forces. Periodic maneuvers are required to keep the satellite in its orbit. The frequency of maneuvers depends primarily on the solar flux as it affects the Earth's atmosphere, and there are expected to be one maneuver (or series of maneuvers) every 40 to 200 days.

Each orbit maintenance maneuver is performed using only one thrust to minimize impacts on the ground orbit solution. Orbit computation is optimized to minimize the orbit error during such periods. Science data are taken during orbit maintenance maneuvers and are distributed (an orbit state flag is provided in the products).



2.4.3.1.1. Equator Crossing Longitudes (in order of Pass Number)

Pass	Longitude										
1	99.9249	44	30.4744	87	321.0274	130	251.5783	173	182.1282	216	112.6813
2	265.7517	45	196.3012	88	126.8541	131	57.4042	174	347.9550	217	278.5075
3	71.5776	46	2.1280	89	292.6810	132	223.2310	175	153.7829	218	84.3343
4	237.4044	47	167.9557	90	98.5078	133	29.0576	176	319.6096	219	250.1600
5	43.2305	48	333.7825	91	264.3336	134	194.8843	177	125.4369	220	55.9867
6	209.0573	49	139.6102	92	70.1603	135	0.7117	178	291.2636	221	221.8129
7	14.8844	50	305.4370	93	235.9862	136	166.5385	179	97.0902	222	27.6397
8	180.7112	51	111.2637	94	41.8130	137	332.3659	180	262.9170	223	193.4666
9	346.5387	52	277.0905	95	207.6395	138	138.1927	181	68.7430	224	359.2934
10	152.3655	53	82.9167	96	13.4663	139	304.0198	182	234.5697	225	165.1212
11	318.1928	54	248.7435	97	179.2937	140	109.8466	183	40.3959	226	330.9479
12	124.0196	55	54.5694	98	345.1205	141	275.6727	184	206.2227	227	136.7755
13	289.8463	56	220.3962	99	150.9484	142	81.4995	185	12.0499	228	302.6023
14	95.6731	57	26.2229	100	316.7751	143	247.3252	186	177.8767	229	108.4290
15	261.4989	58	192.0497	101	122.6022	144	53.1520	187	343.7042	230	274.2558
16	67.3256	59	357.8771	102	288.4290	145	218.9782	188	149.5309	231	80.0819
17	233.1515	60	163.7039	103	94.2556	146	24.8050	189	315.3582	232	245.9087
18	38.9783	61	329.5313	104	260.0823	147	190.6320	190	121.1850	233	51.7347
19	204.8049	62	135.3580	105	65.9083	148	356.4588	191	287.0117	234	217.5614
20	10.6317	63	301.1851	106	231.7351	149	162.2866	192	92.8384	235	23.3883
21	176.4592	64	107.0119	107	37.5614	150	328.1133	193	258.6642	236	189.2150
22	342.2860	65	272.8379	108	203.3881	151	133.9409	194	64.4909	237	355.0425
23	148.1139	66	78.6647	109	9.2154	152	299.7676	195	230.3169	238	160.8693
24	313.9406	67	244.4904	110	175.0422	153	105.5943	196	36.1437	239	326.6966
25	119.7676	68	50.3172	111	340.8697	154	271.4211	197	201.9704	240	132.5234
26	285.5944	69	216.1435	112	146.6964	155	77.2471	198	7.7971	241	298.3504
27	91.4209	70	21.9702	113	312.5237	156	243.0739	199	173.6248	242	104.1772
28	257.2477	71	187.7974	114	118.3505	157	48.8999	200	339.4515	243	270.0031
29	63.0736	72	353.6242	115	284.1770	158	214.7267	201	145.2793	244	75.8299
30	228.9004	73	159.4520	116	90.0038	159	20.5536	202	311.1061	245	241.6556
31	34.7268	74	325.2788	117	255.8295	160	186.3804	203	116.9330	246	47.4824
32	200.5535	75	131.1062	118	61.6562	161	352.2079	204	282.7598	247	213.3088
33	6.3809	76	296.9330	119	227.4823	162	158.0346	205	88.5862	248	19.1355
34	172.2076	77	102.7596	120	33.3090	163	323.8620	206	254.4130	249	184.9628
35	338.0351	78	268.5864	121	199.1358	164	129.6887	207	60.2389	250	350.7896
36	143.8619	79	74.4124	122	4.9626	165	295.5157	208	226.0657	251	156.6174
37	309.6891	80	240.2392	123	170.7903	166	101.3425	209	31.8922	252	322.4442
38	115.5159	81	46.0652	124	336.6170	167	267.1683	210	197.7189	253	128.2715
39	281.3423	82	211.8920	125	142.4448	168	72.9951	211	3.5463	254	294.0983
40	87.1690	83	17.7190	126	308.2716	169	238.8209	212	169.3731		
41	252.9947	84	183.5458	127	114.0984	170	44.6477	213	335.2005		
42	58.8215	85	349.3733	128	279.9252	171	210.4741	214	141.0273		
43	224.6476	86	155.2000	129	85.7515	172	16.3009	215	306.8545		

Table 7 : Equator Crossing Longitudes (in order of Pass Number)



2.4.3.1.2. Equator Crossing Longitudes (in order of Longitude)

Pass	Longitude										
135	0.7117	118	61.6562	101	122.6022	84	183.5458	67	244.4904	50	305.4370
46	2.1280	29	63.0736	12	124.0196	249	184.9628	232	245.9087	215	306.8545
211	3.5463	194	64.4909	177	125.4369	160	186.3804	143	247.3252	126	308.2716
122	4.9626	105	65.9083	88	126.8541	71	187.7974	54	248.7435	37	309.6891
33	6.3809	16	67.3256	253	128.2715	236	189.2150	219	250.1600	202	311.1061
198	7.7971	181	68.7430	164	129.6887	147	190.6320	130	251.5783	113	312.5237
109	9.2154	92	70.1603	75	131.1062	58	192.0497	41	252.9947	24	313.9406
20	10.6317	3	71.5776	240	132.5234	223	193.4666	206	254.4130	189	315.3582
185	12.0499	168	72.9951	151	133.9409	134	194.8843	117	255.8295	100	316.7751
96	13.4663	79	74.4124	62	135.3580	45	196.3012	28	257.2477	11	318.1928
7	14.8844	244	75.8299	227	136.7755	210	197.7189	193	258.6642	176	319.6096
172	16.3009	155	77.2471	138	138.1927	121	199.1358	104	260.0823	87	321.0274
83	17.7190	66	78.6647	49	139.6102	32	200.5535	15	261.4989	252	322.4442
248	19.1355	231	80.0819	214	141.0273	197	201.9704	180	262.9170	163	323.8620
159	20.5536	142	81.4995	125	142.4448	108	203.3881	91	264.3336	74	325.2788
70	21.9702	53	82.9167	36	143.8619	19	204.8049	2	265.7517	239	326.6966
235	23.3883	218	84.3343	201	145.2793	184	206.2227	167	267.1683	150	328.1133
146	24.8050	129	85.7515	112	146.6964	95	207.6395	78	268.5864	61	329.5313
57	26.2229	40	87.1690	23	148.1139	6	209.0573	243	270.0031	226	330.9479
222	27.6397	205	88.5862	188	149.5309	171	210.4741	154	271.4211	137	332.3659
133	29.0576	116	90.0038	99	150.9484	82	211.8920	65	272.8379	48	333.7825
44	30.4744	27	91.4209	10	152.3655	247	213.3088	230	274.2558	213	335.2005
209	31.8922	192	92.8384	175	153.7829	158	214.7267	141	275.6727	124	336.6170
120	33.3090	103	94.2556	86	155.2000	69	216.1435	52	277.0905	35	338.0351
31	34.7268	14	95.6731	251	156.6174	234	217.5614	217	278.5075	200	339.4515
196	36.1437	179	97.0902	162	158.0346	145	218.9782	128	279.9252	111	340.8697
107	37.5614	90	98.5078	73	159.4520	56	220.3962	39	281.3423	22	342.2860
18	38.9783	1	99.9249	238	160.8693	221	221.8129	204	282.7598	187	343.7042
183	40.3959	166	101.3425	149	162.2866	132	223.2310	115	284.1770	98	345.1205
94	41.8130	77	102.7596	60	163.7039	43	224.6476	26	285.5944	9	346.5387
5	43.2305	242	104.1772	225	165.1212	208	226.0657	191	287.0117	174	347.9550
170	44.6477	153	105.5943	136	166.5385	119	227.4823	102	288.4290	85	349.3733
81	46.0652	64	107.0119	47	167.9557	30	228.9004	13	289.8463	250	350.7896
246	47.4824	229	108.4290	212	169.3731	195	230.3196	178	291.2636	161	352.2079
157	48.9999	140	109.8466	123	170.7903	106	231.7351	89	292.6810	72	353.6242
68	50.3172	51	111.2637	34	172.2076	17	233.1515	254	294.0983	237	355.0425
233	51.7347	216	112.6813	199	173.6248	182	234.5697	165	295.5157	148	356.4588
144	53.1520	127	114.0984	110	175.0422	93	235.9862	76	296.9330	59	357.8771
55	54.5694	38	115.5159	21	176.4592	4	237.4044	241	298.3504	224	359.2934
220	55.9867	203	116.9330	186	177.8767	169	238.8209	152	299.7676		
131	57.4042	114	118.3505	97	179.2937	80	240.2392	63	301.1851		
42	58.8215	25	119.7676	8	180.7112	245	241.6556	228	302.6023		
207	60.2389	190	121.1850	173	182.1282	156	243.0739	139	304.0198		

Table 8 : Equator Crossing Longitudes (in order of Longitude)



### 2.4.3.2. Repetitive orbit on interleaved orbit (October 2016-July 2017)

After approval by the Joint Steering Group (held on 12 Sept 2016), the OSTM/Jason-2 satellite was moved to a new ground track early October 2016 after the end of repeat cycle 303, after more than 8 years of service on the nominal ground track.

The satellite was moved to the same interleaved orbit that was used by Topex from 2002-2005 and Jason-1 from 2009-2012. Several maneuvers were performed between October 2<sup>nd</sup>, 2016, and October 14<sup>th</sup>, 2016.

Regarding the interleaved OSTM/Jason-2 orbit.

- OSTM/Jason-2 uses the same pass numbering scheme adopted by Topex and Jason-1 in the interleaved ground track. However, the start time of the OSTM/Jason-2 and Jason-3 repeat cycles differs by approximately 5 days.
- The first OSTM/Jason-2 repeat cycle on the new interleaved ground track is cycle 305.
- The OSTM/Jason-2 altimeter was placed in wait mode and data production (OGDR, IGDR and GDR) was stopped during the transit to the interleaved orbit. It was restarted during cycle 305 with the same requirements for data latency and quality.

#### 2.4.3.2.1. Equator Crossing Longitudes (in order of Pass Number)

Pass	Longitude										
1	98.51	44	29.06	87	319.62	130	250.17	173	180.72	216	111.27
2	264.34	45	194.89	88	125.44	131	55.99	174	346.55	217	277.10
3	70.17	46	0.72	89	291.27	132	221.82	175	152.37	218	82.92
4	235.99	47	166.54	90	97.10	133	27.65	176	318.20	219	248.75
5	41.82	48	332.37	91	262.92	134	193.48	177	124.03	220	54.58
6	207.65	49	138.20	92	68.75	135	359.30	178	289.85	221	220.40
7	13.47	50	304.03	93	234.57	136	165.13	179	95.68	222	26.23
8	179.30	51	109.85	94	40.40	137	330.95	180	261.51	223	192.06
9	345.13	52	275.68	95	206.23	138	136.78	181	67.33	224	357.89
10	150.96	53	81.51	96	12.06	139	302.61	182	233.16	225	163.71
11	316.78	54	247.33	97	177.88	140	108.44	183	38.99	226	329.54
12	122.61	55	53.16	98	343.71	141	274.26	184	204.81	227	135.36
13	288.43	56	218.99	99	149.54	142	80.09	185	10.64	228	301.19
14	94.26	57	24.81	100	315.37	143	245.91	186	176.47	229	107.02
15	260.09	58	190.64	101	121.19	144	51.74	187	342.29	230	272.85
16	65.92	59	356.47	102	287.02	145	217.57	188	148.12	231	78.67
17	231.74	60	162.29	103	92.84	146	23.40	189	313.95	232	244.50
18	37.57	61	328.12	104	258.67	147	189.22	190	119.78	233	50.32
19	203.39	62	133.95	105	64.50	148	355.05	191	285.60	234	216.15
20	9.22	63	299.77	106	230.33	149	160.88	192	91.43	235	21.98
21	175.05	64	105.60	107	36.15	150	326.71	193	257.25	236	187.81
22	340.88	65	271.43	108	201.98	151	132.53	194	63.08	237	353.63
23	146.70	66	77.25	109	7.80	152	298.36	195	228.91	238	159.46
24	312.53	67	243.08	110	173.63	153	104.18	196	34.73	239	325.29
25	118.36	68	48.91	111	339.46	154	270.01	197	200.56	240	131.11
26	284.18	69	214.73	112	145.29	155	75.84	198	6.39	241	296.94
27	90.01	70	20.56	113	311.11	156	241.66	199	172.21	242	102.77
28	255.84	71	186.39	114	116.94	157	47.49	200	338.04	243	268.59
29	61.66	72	352.22	115	282.77	158	213.32	201	143.87	244	74.42
30	227.49	73	158.04	116	88.59	159	19.14	202	309.70	245	240.24



31	33.32	74	323.87	117	254.42	160	184.97	203	115.52	246	46.07
32	199.14	75	129.69	118	60.25	161	350.80	204	281.35	247	211.90
33	4.97	76	295.52	119	226.07	162	156.63	205	87.18	248	17.73
34	170.80	77	101.35	120	31.90	163	322.45	206	253.00	249	183.55
35	336.62	78	267.18	121	197.72	164	128.28	207	58.83	250	349.38
36	142.45	79	73.00	122	3.55	165	294.10	208	224.66	251	155.21
37	308.28	80	238.83	123	169.38	166	99.93	209	30.48	252	321.04
38	114.11	81	44.65	124	335.21	167	265.76	210	196.31	253	126.86
39	279.93	82	210.48	125	141.03	168	71.59	211	2.14	254	292.69
40	85.76	83	16.31	126	306.86	169	237.41	212	167.96		
41	251.58	84	182.14	127	112.69	170	43.24	213	333.79		
42	57.41	85	347.96	128	278.52	171	209.06	214	139.62		
43	223.24	86	153.79	129	84.34	172	14.89	215	305.44		

Table 9 : Equator Crossing Longitudes (in order of Pass Number)

2.4.3.2.2. Equator Crossing Longitudes (in order of Longitude)

Pass	Longitude										
46	0.72	29	61.66	12	122.61	249	183.55	232	244.50	215	305.44
211	2.14	194	63.08	177	124.03	160	184.97	143	245.91	126	306.86
122	3.55	105	64.50	88	125.44	71	186.39	54	247.33	37	308.28
33	4.97	16	65.92	253	126.86	236	187.81	219	248.75	202	309.70
198	6.39	181	67.33	164	128.28	147	189.22	130	250.17	113	311.11
109	7.80	92	68.75	75	129.69	58	190.64	41	251.58	24	312.53
20	9.22	3	70.17	240	131.11	223	192.06	206	253.00	189	313.95
185	10.64	168	71.59	151	132.53	134	193.48	117	254.42	100	315.37
96	12.06	79	73.00	62	133.95	45	194.89	28	255.84	11	316.78
7	13.47	244	74.42	227	135.36	210	196.31	193	257.25	176	318.20
172	14.89	155	75.84	138	136.78	121	197.72	104	258.67	87	319.62
83	16.31	66	77.25	49	138.20	32	199.14	15	260.09	252	321.04
248	17.73	231	78.67	214	139.62	197	200.56	180	261.51	163	322.45
159	19.14	142	80.09	125	141.03	108	201.98	91	262.92	74	323.87
70	20.56	53	81.51	36	142.45	19	203.39	2	264.34	239	325.29
235	21.98	218	82.92	201	143.87	184	204.81	167	265.76	150	326.71
146	23.40	129	84.34	112	145.29	95	206.23	78	267.18	61	328.12
57	24.81	40	85.76	23	146.70	6	207.65	243	268.59	226	329.54
222	26.23	205	87.18	188	148.12	171	209.06	154	270.01	137	330.95
133	27.65	116	88.59	99	149.54	82	210.48	65	271.43	48	332.37
44	29.06	27	90.01	10	150.96	247	211.90	230	272.85	213	333.79
209	30.48	192	91.43	175	152.37	158	213.32	141	274.26	124	335.21
120	31.90	103	92.84	86	153.79	69	214.73	52	275.68	35	336.62
31	33.32	14	94.26	251	155.21	234	216.15	217	277.10	200	338.04
196	34.73	179	95.68	162	156.63	145	217.57	128	278.52	111	339.46
107	36.15	90	97.10	73	158.04	56	218.99	39	279.93	22	340.88
18	37.57	1	98.51	238	159.46	221	220.40	204	281.35	187	342.29
183	38.99	166	99.93	149	160.88	132	221.82	115	282.77	98	343.71
94	40.40	77	101.35	60	162.29	43	223.24	26	284.18	9	345.13
5	41.82	242	102.77	225	163.71	208	224.66	191	285.60	174	346.55



170	43.24	153	104.18	136	165.13	119	226.07	102	287.02	85	347.96
81	44.65	64	105.60	47	166.54	30	227.49	13	288.43	250	349.38
246	46.07	229	107.02	212	167.96	195	228.91	178	289.85	161	350.80
157	47.49	140	108.44	123	169.38	106	230.33	89	291.27	72	352.22
68	48.91	51	109.85	34	170.80	17	231.74	254	292.69	237	353.63
233	50.32	216	111.27	199	172.21	182	233.16	165	294.10	148	355.05
144	51.74	127	112.69	110	173.63	93	234.57	76	295.52	59	356.47
55	53.16	38	114.11	21	175.05	4	235.99	241	296.94	224	357.89
220	54.58	203	115.52	186	176.47	169	237.41	152	298.36	135	359.30
131	55.99	114	116.94	97	177.88	80	238.83	63	299.77		
42	57.41	25	118.36	8	179.30	245	240.24	228	301.19		
207	58.83	190	119.78	173	180.72	156	241.66	139	302.61		
118	60.25	101	121.19	84	182.14	67	243.08	50	304.03		

Table 10 : Equator Crossing Longitudes (in order of Longitude)

### 2.4.3.3. Repetitive orbit on Long Repeat orbit (July 2017-July 2018)

After approval by the Joint Steering Group (held on 20 July 2017), the OSTM/Jason-2 satellite was moved to a new orbit and ground track in July 2017 after the end of repeat cycle 326 (and 2 months of unavailability due to on board incident), after 9 years of service.

The satellite was moved to an orbit 27km under the nominal one (i.e. at 1309km altitude), known as the “Long Repeat Orbit”, with a cycle of nearly 368 days (composed of 4736 revolutions). This orbit can also be defined with no ambiguity with the following phased orbit parameters [N,P,Q] = [12,284,371], with the same inclination as the original orbit (66.042°). Several maneuvers were performed between July 3<sup>rd</sup>, 2017, and July 10<sup>th</sup>, 2017.

Regarding the LRO OSTM/Jason-2 orbit.

- OSTM/Jason-2 still (artificially) uses the same pass numbering scheme as on the original orbit, i.e. 254 passes on a nearly 10-days cycle.
- The first OSTM/Jason-2 repeat cycle on the LRO ground track is cycle 500.
- The OSTM/Jason-2 altimeter was placed in wait mode and data production (OGDR, IGDR and GDR) was stopped from May 17<sup>th</sup> 2017 until the transit to the interleaved orbit. It was restarted during cycle 500 with the same requirements for data latency and quality.

### 2.4.3.4. Repetitive orbit on Interleaved Long Repeat orbit (July 2018-Oct 2019)

After approval by the Joint Steering Group (held on 24 May 2018), the OSTM/Jason-2 satellite was moved from LRO to an interleaved LRO orbit in the middle of the grid already defined on Earth by the LRO. This was done by translating the ground track of 4km. All conventions (cycle number...) and orbit parameters remained the same as on LRO. This so-called “i-LRO orbit” is defined by the same parameters as LRO, and changing the longitude of the 1<sup>st</sup> ascending node (on 18/07/2018 at 13h48m11s000) with the following value: 225.34527212 degrees. Cycles are restarted from number 600 on 2018/07/18 at 13:20:12. This orbit was used until the end of the mission the October 1<sup>st</sup>, 2019

## 2.4.4. The OSTM/Jason-2 Project Phases

The satellite mission has two phases:

The calibration/validation phase (9 months) began shortly after launch, when the satellite reached the operational (nominal repetitive) orbit and the satellite and sensor systems were functioning normally. This phase continued until the data received from the sensors were satisfactorily calibrated and verified. Unlike Jason-1, the Cal/Val phase is divided in 2 phases which overlap:

1. One dedicated to the validation of the near real time products (OGDRs). An OSTST meeting in November 2008 was organized to validate those products and to provide the validation status required to allow data dissemination to end users. Since Jason-1 was to be moved to



the interleaved orbit in early 2009, and taking into account the very good data quality of Jason-2 IGDR products, it was also decided to disseminate IGDR off-line products to end users in January 2009.

2. The second phase was dedicated to the validation of the off-line products (IGDR and GDR). An OSTST meeting in June 2009 was organized to validate those products and to provide the validation status required to allow data dissemination to end users.

The operational phase begins after the successful validation of each product type, and when all necessary algorithm and processing changes are implemented to have OSTM/Jason-2 performances at the same level as Jason-1.

## 2.5. Data Processing and Distribution

---

Processing centers perform functions such as science data processing, data verification and orbit determination.

There are three levels of processed data:

- Telemetry data (raw data or level0)
- Sensor Data Records (engineering units or level1)
- Geophysical Data Records (geophysical units or level2)

There are two kinds of data processing and distribution:

- Real-time processing and distribution (EUMETSAT and NOAA): not applicable to GDR-F.

The operational geophysical data record (OGDR) is available with a latency of 3-5 hours. Note that this is a non-validated product that uses orbits computed by the on-board DORIS Navigator (DIODE) and that it does not contain all the environmental/geophysical corrections.

- Delayed-mode processing (CNES) and distribution (CNES and NOAA)

The interim geophysical data record (IGDR) is available per pass with a latency of 2 days. Note that this is not a fully validated product, although it uses a preliminary orbit and includes all the environmental/geophysical corrections (preliminary for some of them). IGDR is not applicable to GDR-F.

The geophysical data record (GDR) is a fully validated product that uses a precise orbit and the best environmental/geophysical corrections. This product is available per repeat cycle with a latency of 90 days. Validation is performed by two teams at CNES and NASA/JPL to ensure in depth validation.

Geophysical data records are disseminated to users as they become available, as well as ingested in two main archives (at CNES and NOAA), where they are made available to the scientific community.

The NRT and offline data are provided through different sources and means as discussed below. Note that the telemetry acquisition strategy, designed to minimize the risk of science data loss, sometimes results in files containing data which overlaps in time. The NRT ground processing does not remove these overlaps, so it is possible to encounter two or more OGDR products which have overlapping start and stop sensing times. CNES-EUMETSAT-NOAA centers are disseminating Jason-2 products according to the interagency agreement.

- CNES via AVISO+ data services: <http://www.aviso.altimetry.fr>

“Archiving, Validation and Interpretation of Satellite Oceanographic data” is the French multi-satellite data distribution center dedicated to space oceanography, developed by CNES.

AVISO+ distributes and archives Jason-2 delayed-time data ((I)GDR).

- EUMETSAT: <http://www.eumetsat.int>

EUMETSAT is the European Organisation for the Exploitation of Meteorological Satellites. Its role is to deliver weather and climate-related satellite data, images and products- 24 hours a day, 365



days a year.

EUMETSAT distributes operational data (OGDR)

- NOAA: <http://www.noaa.gov>

The mission of the US National Oceanic and Atmospheric Administration is to understand and predict changes in Earth's environment and conserve and manage coastal and marine resources to meet USA's economic, social, and environmental needs

NOAA distributes operational data, and distributes and archives delayed-time data ((O)(I)GDR)

## 2.5.1. Access to NRT data

This paragraph is not applicable to GDR-F

The OGDR, OGDR-SSHA, and OGDR-BUFR files are produced at NOAA and EUMETSAT. Telemetry data downlinked to NOAA's ground stations at Wallops, VA and Fairbanks, AK are used to produce NOAA OGDR products, while telemetry data downlinked to the EUMETSAT earth terminal at Usingen, Germany are used to produce EUMETSAT OGDRs. NOAA and EUMETSAT exchange their products so that both agencies have a complete set.

In near real time, NOAA disseminates the complete set of OGDR files via ftp and EUMETSAT disseminates the complete set of OGDR files on EUMETCast. The complete set of OGDR files consists of OGDR, OGDR-SSHA and OGDR-BUFR, both generated at EUMETSAT and NOAA.

Note that the OGDR-BUFR files available from NOAA/CLASS use a filename similar to the native and reduced-SSHA filenames, beginning with 'JA2\_OPB'. The UMARF archive at EUMETSAT utilizes the WMO/GTS filenames indicated above, beginning with 'W\_US' for NOAA OGDR-BUFR files and 'W\_XX' for the EUMETSAT generated OGDR-BUFR files.

The OGDR-BUFR data are additionally available in near real-time from the Global Telecommunications System (GTS). NOAA and EUMETSAT inject only their own OGDR-BUFR files onto GTS, to avoid duplication.

Details on data dissemination services from NOAA and EUMETSAT agencies are described below.

## 2.5.2. Access to off-line data

The IGDR and GDR families of files are produced solely by CNES, and are available to users from NOAA's National Centers for Environmental Information (NCEI);

<https://www.ncei.noaa.gov/products/jason-satellite-products>), and from the French Archiving, Validation, and Interpretation of Satellite Oceanographic data (AVISO; <http://www.aviso.altimetry.fr>) ftp server. Both of these archival facilities also provide a variety of auxiliary files used to produce the O/I/GDR datasets, and NOAA also provides the OGDR family of datasets.

Data dissemination services from NOAA and CNES agencies are described below.

## 2.5.3. Documentation

This Jason-2 User's Handbook document describes only the native product format. A description of the O/I/GDR product format and contents is provided in the CNES document "SALP-ST-M-EA-15704-CN: SALP Products Specification - Volume 1: Jason-2 User Products". All documents are available through the data dissemination services.

A BUFR reading software library can be obtained from:  
<http://www.ecmwf.int/products/data/software/bufr.html>

## 2.6. Access to data via NOAA

---

### 2.6.1. Access to NRT data

This paragraph is not applicable to GDR-F



---

Individual users who require science data in near-real-time can access the O/I/GDR at the National Centers for Environmental Information (NCEI): <https://www.ncei.noaa.gov/products/jason-satellite-products> . Supported access methods include direct ftp, http, and OPeNDAP and THREDDS. Helpdesk support is available during normal business hours via [NCEI.services@noaa.gov](mailto:NCEI.services@noaa.gov). The NCEI Satellite Oceanography team can help users create subscriptions to specified data streams as well as provide access to ancillary, auxiliary, orbital and other types of Jason-3 data.

Operational users who demonstrate a need for minimum latency near real-time access will need to register with NOAA's Product Distribution & Access server (PDA). Please contact the PDA administrator ([PDA\\_Administrator@noaa.gov](mailto:PDA_Administrator@noaa.gov)) to determine if PDA access is needed for your use. Online registration will be provided once approval has been given to use the PDA.

## 2.7. Access to data via EUMETSAT

---

### 2.7.1. NRT data access

This paragraph is not applicable to GDR-F

Operational users requiring near real-time access (within a few hours of acquisition) can receive data via EUMETCast, which is the prime dissemination mechanism for EUMETSAT satellite data and meteorological products. EUMETCast is also used to deliver data supplied by several external data providers.

Information on EUMETCast can be found at: <https://www.eumetsat.int>

The Jason-2 products available via EUMETCast are the EUMETSAT and NOAA injected OGDR, OGDR-SSHA and OGDR-BUFR. To access these on EUMETCast, users should register via the Earth Observation Portal (<https://eoportal.eumetsat.int/>).

All enquiries related to EUMETCast can be addressed to the EUMETSAT User Helpdesk, email [ops@eumetsat.int](mailto:ops@eumetsat.int), who will be happy to assist with information on reception station manufacturers, reception station setup and data access registration to the Jason-2 service, or indeed to other near real-time EUMETSAT data services.

### 2.7.2. Access to archived data

The Jason-2 products generated and distributed by EUMETSAT in near real-time (i.e., OGDR, OGDR-SSHA and OGDR-BUFR) are also archived in the multi-mission EUMETSAT Data Center. Any user can access Jason-3 data from the EUMETSAT Data Center upon registration. Information on registration, the Data Center itself and how to use it can be found at <https://www.eumetsat.int>. Note however that this is not a near real-time data access, but that it can take up to several hours and occasionally even days to get the data.

## 2.8. Access to for OGDR-BUFR data on GTS

---

This paragraph is not applicable to GDR-F

## 2.9. CNES data distribution

---

### 2.9.1. Details of off line data access via CNES

Off line IGDR and GDR products via **Aviso+ ftp portal with an authenticated access (<ftp://ftp-access.aviso.altimetry.fr/>)**.

Registration is needed : <https://www.aviso.altimetry.fr/en/data/data-access/registration-form.html> and select the products

- o “GDR / IGDR (Geophysical Data Records)” and/or
- o “Waveform (Radar return echoes in Sensor Geophysical Data Records)” and/or



o “Wind / Wave Along-track from Geophysical Data Records (L2)”, depending on the way you use them.

A login/password are provided .

Home directory : /geophysical-data-record/jason-2

With the following ftp server directory tree:

- documentation → directory containing product spec, product handbook, reading tools, ...
- gdr\_d → directory containing D-Standard GDR native products  
(with a sub directory for each cycle)
- sgdr\_d → directory containing D-Standard S-GDR  
(with a sub directory for each cycle)
- ssha\_gdr\_d → directory containing D-Standard GDR reduced products  
(with a sub directory for each cycle)
- gdr\_f → directory containing F-Standard GDR native products  
(with a sub directory for each cycle)
- sgdr\_f → directory containing F-Standard S-GDR  
(with a sub directory for each cycle)
- ssha\_gdr\_f → directory containing F-Standard GDR reduced products  
(with a sub directory for each cycle)
- gdr\_d\_validation\_report → directory containing GDR-D validation reports

For any questions on Jason-2 data dissemination on AVISO+ servers please contact:

[aviso@altimetry.fr](mailto:aviso@altimetry.fr)



### 3. Product evolution history

#### 3.1. Models and Standards History

##### 3.1.1. GDR Product Version "T" and O/IGDR Product Version "c"

###### 3.1.1.1. Models and Standards

The version of the data produced during the Cal/Val phase of the Jason-2 mission is identified by the version letter "T" in the name of the data products.

This product version adopts models and standards that are consistent with version "c" of the Jason-1 (I)GDR products (see RD 2). Since the OSTST meeting held in November 2008, OGDR and IGDR products are available to end users and identified by the version letter "c" in the name of the data products. The version 'T' calibration/validation GDRs have been extensively validated by the Ocean Surface Topography Science Team (OSTST) during the OSTST meeting held in June 2009, who found that these GDRs are demonstrating excellent data quality, and consistency with the Jason-1 version 'c' GDRs. The OSTST recommended so release of the Jason-2/OSTM Version 'T' GDRs as is. There are a few known minor issues with some fields in the version 'T' GDRs (see Jason-2 GDR\_T release note). These issues are corrected in the Jason-2 version 'd' GDRs.

The table below summarizes the models and standards that are adopted in this version of the OSTM/Jason-2 (O)(I)GDRs. Section 3.2 provides more details on some of these models.

Model	GDR Product Version "T" and O/IGDR Product Version "c"
Orbit	Based on Doris onboard navigator solution for OGDRS. DORIS tracking data for IGDRs DORIS+SLR+GPS tracking data for GDRs.
Altimeter Retracking	<p><u>"Ocean" retracking</u> MLE4 fit from 2<sup>nd</sup> order Brown analytical model : MLE4 simultaneously retrieves the 4 parameters that can be inverted from the altimeter waveforms:</p> <ul style="list-style-type: none"> <li>- Epoch (tracker range offset) <math>\Rightarrow</math> altimeter range</li> <li>- Composite Sigma <math>\Rightarrow</math> SWH</li> <li>- Amplitude <math>\Rightarrow</math> Sigma0</li> <li>- Square of mispointing angle (Ku band only, a null value is used in input of the C band retracking algorithm)</li> </ul> <p><u>"Ice" retracking</u> Geometrical analysis of the altimeter waveforms, which retrieves the following parameters:</p> <ul style="list-style-type: none"> <li>- Epoch (tracker range offset) <math>\Rightarrow</math> altimeter range</li> <li>- Amplitude <math>\Rightarrow</math> Sigma0</li> </ul>
Altimeter Instrument Corrections	Consistent with MLE4 retracking algorithm
Jason-2 Advanced Microwave Radiometer (AMR) Parameters	Using calibration parameters derived from long term calibration tool developed and operated by NASA/JPL
Dry Troposphere Range Correction	From ECMWF atmospheric pressures and model for S1 and S2 atmospheric tides
Wet Troposphere Range Correction from Model	From ECMWF model
Ionosphere correction	Based on Global Ionosphere TEC Maps from JPL
Sea State Bias	Empirical model derived from 3 years of MLE4 Jason-1 altimeter data with version "b" geophysical models



Model	GDR Product Version "T" and O/IGDR Product Version "c"
Mean Sea Surface	CLS01
Mean Dynamic Topography	CLS Rio 05
Geoid	EGM96
Bathymetry Model	DTM2000.1
Inverse Barometer Correction	Computed from ECMWF atmospheric pressures after removing S1 and S2 atmospheric tides
Non-tidal High-frequency Dealiasing Correction	Mog2D High Resolution ocean model on (I)GDRs. None for OGDRs. Ocean model forced by ECMWF atmospheric pressures after removing S1 and S2 atmospheric tides
Tide Solution 1	GOT00.2 + S1 ocean tide . S1 load tide ignored
Tide Solution 2	FES2004 + S1 and M4 ocean tides. S1 and M4 load tides ignored
Equilibrium long-period ocean tide model	From Cartwright and Taylor tidal potential
Non-equilibrium long-period ocean tide model	Mm, Mf, Mtm, and Msqm from FES2004
Solid Earth Tide Model	From Cartwright and Taylor tidal potential
Pole Tide Model	Equilibrium model
Wind Speed from Model	ECMWF model
Altimeter Wind Speed Model	Derived from TOPEX/POSEIDON data
Rain Flag	Derived from comparisons to thresholds of the radiometer-derived integrated liquid water content and of the difference between the measured and the expected Ku-band AGCs
Ice Flag	Derived from comparison of the model wet tropospheric correction to a dual-frequency wet tropospheric correction retrieved from radiometer brightness temperatures, with a default value issued from a climatology table

**Table 11** : Models and standards (Jason-2 GDR Product Version "T" and O/IGDR Product Version "c")

### 3.1.1.2. Sea Surface Height Bias

The estimate of the absolute bias in the OSTM/Jason-2 sea-surface height measurements (SSH) is one of the goals of the Cal/Val phase and was therefore not fully consolidated.

The CalVal studies show a JA2 absolute range difference of the order of 17.0 cm during the tandem phase, obtained from global analyses or from the in-situ CalVal sites. Most of this range bias comes from an error in some parameterization files Jason-2 discovered by the project before the Seattle OSTST meeting in June 2009. There are 2 main components which contribute to this bias:

- A lack of accuracy of the altimeter PRF (Pulse Repetition Frequency) that is applied today in the ground segment (truncation effect). If applied correctly, the JA2 range will be shortened by 25 mm, so increasing the absolute bias to 19.5 cms.
- A wrong antenna reference point for the computation of the Jason-2 range. If applied correctly, the JA2 range will be increased by 180 mm, so decreasing the absolute bias to about 1.5 cms.

These two errors (Jason-2 PRF value and antenna reference point) are corrected in the Jason-2 GDR-D products version.

### 3.1.1.3. Time-tag Bias

The long period crossover point residual analysis show a datation bias about 250µs, leading to a sea surface height anomaly (SSHA) error varying with latitudes. The origin of the error has been precisely determined and its value can be retrieve by the following formula:

$$\text{Time tag bias} = RA \times PRI - 2 \times \text{alt}/c$$

Where :

- Time tag bias = datation bias



- RA = ambiguity order (=18)
- PRI = Pulse Repetition Frequency (=1/2058.513239)
- alt = satellite altitude
- c = celerity

This datation bias is corrected in the Jason-2 GDR-D product version.

### 3.1.2. Version "d" Products

#### 3.1.2.1. Models and Standards

The current product version corrects a few minor issues in the version 'T' GDRs, adopts some new models, and account for inclusion of MLE-3 retracking parameters and new radiometer fields improving the coastal data quality.

The table below summarizes the models and standards that are adopted in this version of the OSTM/Jason-2 (O)(I)GDRs. Section 3.2 provides more details on some of these models.

Model	Product Version "d"
Orbit	<ul style="list-style-type: none"> <li>- Based on Doris onboard navigator solution for OGDRS.</li> <li>- DORIS tracking data for IGDRs (orbit standard "GRD-D" until cycle 253 included and orbit standard "GRD-E" from cycle 254).</li> <li>- DORIS+SLR+GPS tracking data for GDRs until cycle 253 included (orbit standard "GRD-D").</li> <li>- DORIS and/or SLR and/or GPS tracking data for GDRs from cycle 254 (orbit standard "GRD-E").</li> </ul>
Altimeter Retracking	<p><u>"Ocean MLE4" retracking</u> MLE4 fit from 2<sup>nd</sup> order Brown analytical model : MLE4 simultaneously retrieves the 4 parameters that can be inverted from the altimeter waveforms:</p> <ul style="list-style-type: none"> <li>- Epoch (tracker range offset) ⇒ altimeter range</li> <li>- Composite Sigma ⇒ SWH</li> <li>- Amplitude ⇒ Sigma0</li> <li>- Square of mispointing angle (Ku band only, a null value is used in input of the C band retracking algorithm)</li> </ul> <p><u>"Ocean MLE3" retracking</u> MLE3 fit from 1<sup>st</sup> order Brown analytical model : MLE3 simultaneously retrieves the 3 parameters that can be inverted from the altimeter waveforms:</p> <ul style="list-style-type: none"> <li>- Epoch (tracker range offset) ⇒ altimeter range</li> <li>- Composite Sigma ⇒ SWH</li> <li>- Amplitude ⇒ Sigma0</li> </ul> <p><u>"Ice" retracking</u> Geometrical analysis of the altimeter waveforms, which retrieves the following parameters:</p> <ul style="list-style-type: none"> <li>- Epoch (tracker range offset) ⇒ altimeter range</li> <li>- Amplitude ⇒ Sigma0</li> </ul>
Altimeter Instrument Corrections	<p>Two sets:</p> <ul style="list-style-type: none"> <li>- one set consistent with MLE4 retracking</li> <li>- one set consistent with MLE3 retracking</li> </ul>
Jason-2 Advanced Microwave Radiometer (AMR) Parameters	Using calibration parameters derived from long term calibration tool developed and operated by NASA/JPL



Model	Product Version “d”
Dry Troposphere Range Correction	From ECMWF atmospheric pressures and model for S1 and S2 atmospheric tides
Wet Troposphere Range Correction from Model	From ECMWF model
Ionosphere correction	Based on Global Ionosphere TEC Maps from JPL
Sea State Bias	Two empirical models: <ul style="list-style-type: none"> <li>- MLE4 version derived from 1 year of MLE4 Jason-2 altimeter data with version "d" geophysical models</li> <li>- MLE3 version derived from 1 year of MLE3 Jason-2 altimeter data with version "d" geophysical models</li> </ul>
Mean Sea Surface	MSS_CNES-CLS11 MSS_CNES_CLS15 from cycle 500 onwards (on LRO and i-LRO)
Mean Dynamic Topography	MDT_CNES-CLS09
Geoid	EGM96
Bathymetry Model	DTM2000.1
Inverse Barometer Correction	Computed from ECMWF atmospheric pressures after removing S1 and S2 atmospheric tides
Non-tidal High-frequency Dealiasing Correction	Mog2D High Resolution ocean model on (I)GDRs. None for OGDRs. Ocean model forced by ECMWF atmospheric pressures after removing S1 and S2 atmospheric tides
Tide Solution 1	GOT4.8 + S1 ocean tide. S1 load tide ignored
Tide Solution 2	FES2004 + S1 and M4 ocean tides. S1 and M4 load tides ignored
Equilibrium long-period ocean tide model	From Cartwright and Taylor tidal potential
Non-equilibrium long-period ocean tide model	Mm, Mf, Mtm, and Msqm from FES2004
Solid Earth Tide Model	From Cartwright and Taylor tidal potential
Pole Tide Model	Equilibrium model
Wind Speed from Model	ECMWF model
Altimeter Wind Speed Model	Derived from Jason-1 data
Rain Flag	Derived from comparisons to thresholds of the radiometer-derived integrated liquid water content and of the difference between the measured and the expected Ku-band backscatter coefficient
Ice Flag	Derived from comparison of the model wet tropospheric correction to a dual-frequency wet tropospheric correction retrieved from radiometer brightness temperatures, with a default value issued from a climatology table

Table 12 : Version “d” models and standards

### 3.1.2.2. Sea Surface Height Bias

The precise estimate of the absolute bias in the OSTM/Jason-2 sea-surface height measurements (SSH) will be performed after the reprocessing of GDR-D products thanks to in-situ analysis and comparison to Jason-1 data during the formation flying phase. User shall refer to the project web servers for further information.

It should be noted that the bias reflects the combination of the mean errors from all of the corrections that are used to compute sea surface height. The bias provided is intended for sea surface height measurements that are computed with the standard (O)(I)GDR corrections.

### 3.1.3. Standard version "f" Products

The “f” standard version brings major improvements to the previous version 'D' GDRs, adopts some new models, and accounts for inclusion of new fields improving the data quality. The table below summarizes the models and standards that are adopted in this version of the (O)(I)GDRs.



Only GDRs are available in “f” standard (not OGDR nor IGDR).

Model	Product Version “f”
<b>Reference Ellipsoid</b>	WGS84
<b>Orbit</b>	Based on Doris onboard navigator solution for OGDRs. DORIS and/or GPS tracking data for GDRs (orbit standard “POE-F”).
<b>Altimeter Retracking</b>	<p><u>“Ocean MLE4” retracking</u> MLE4 fit from 2<sup>nd</sup> order Brown analytical model : MLE4 simultaneously retrieves the 4 parameters that can be inverted from the altimeter waveforms:</p> <ul style="list-style-type: none"> <li>- Epoch (tracker range offset) ⇒ altimeter range</li> <li>- Composite Sigma ⇒ SWH</li> <li>- Amplitude ⇒ Sigma0</li> <li>- Square of mispointing angle (Ku band only, a null value is used in input of the C band retracking algorithm)</li> </ul> <p><u>“Ocean MLE3” retracking</u> MLE3 fit from 1<sup>st</sup> order Brown analytical model : MLE3 simultaneously retrieves the 3 parameters that can be inverted from the altimeter waveforms:</p> <ul style="list-style-type: none"> <li>- Epoch (tracker range offset) ⇒ altimeter range</li> <li>- Composite Sigma ⇒ SWH</li> <li>- Amplitude ⇒ Sigma0</li> </ul> <p><u>“Ice” retracking</u> Geometrical analysis of the altimeter waveforms, which retrieves the following parameters:</p> <ul style="list-style-type: none"> <li>- Epoch (tracker range offset) ⇒ altimeter range</li> <li>- Amplitude ⇒ Sigma0</li> </ul> <p><u>“Adaptive” retracking</u> Adaptive retracking [Thibaut 2021] fit from Brown numerical model taking the real on-board PTR. Adaptive simultaneously retrieves the 4 parameters that can be inverted from the altimeter waveforms:</p> <ul style="list-style-type: none"> <li>- Epoch (tracker range offset) ⇒ altimeter range</li> <li>- Composite Sigma ⇒ SWH</li> <li>- Amplitude ⇒ Sigma0</li> <li>- Gamma</li> </ul>
<b>Altimeter Instrument Corrections</b>	Two sets: <ul style="list-style-type: none"> <li>- one set consistent with MLE4 retracking</li> <li>- one set consistent with MLE3 retracking</li> </ul> No set needed for adaptive retracking
<b>Jason-3 Advanced Microwave Radiometer (AMR) Parameters</b>	Using calibration parameters derived from long term calibration tool developed and operated by NASA/JPL
<b>Dry Troposphere Range Correction</b>	From ECMWF atmospheric pressures and model for S1 and S2 atmospheric tides. 2 solutions: integration from sea surface level or from estimated measurement altitude using altimetry range (GDR).
<b>Wet Troposphere Range Correction from Model</b>	From ECMWF model. 2 solutions: integration from DEM or using altimetry range.
<b>Ionosphere correction</b>	Two solutions: <ul style="list-style-type: none"> <li>-from Ku/C range differences correction</li> <li>-from Ku/C range differences filtered correction</li> </ul>
<b>Ionosphere model correction</b>	Based on Global Ionosphere TEC Maps from JPL



Model	Product Version “f”
Sea State Bias	CLS empirical solutions fitted on one year of Jason-3 GDR-F data [Tran, 2019] Two solutions for each retracking (MLE4 and Adaptive): - 2D model from SWH and altimeter wind-speed (standard version) - 3D model from SWH, altimeter wind-speed and t02 mean wave period from model (improved version)
Mean Sea Surface	2 Solutions: MSS_CNES-CLS15 MSS_DTU_2018
Mean Dynamic Topography	MDT_CNES-CLS18
Geoid	EGM2008
Bathymetry Model	ACE2 (from EAPRS Laboratory)
Inverse Barometer Correction	Computed from ECMWF atmospheric pressures after removing S1 and S2 atmospheric tides
Non-tidal High-frequency Dealiasing Correction	Mog2D High Resolution ocean model. Ocean model is forced by ECMWF wind field and atmospheric pressure after removing S1 and S2 atmospheric tides
Tide Solution 1	GOT4.10c
Tide Solution 2	FES2014b
Equilibrium long-period ocean tide model	From tidal potential of [Cartwright, 1973]
Non-equilibrium long-period ocean tide model	Mm, Mf, Mtm, MSqm, Sa and Ssa from FES2014b
Solid Earth Tide Model	From tidal potential of [Cartwright, 1973]
Pole Tide Model	From [Desai, 2015] and MPL [Desai, 2017]
Internal Tide Model	From [Zaron, 2019]
Wind Speed from Model	ECMWF model
Altimeter Wind Speed Model	Following Gourrion’s approach [Gourrion, 2000] , based on Collard’s model computed from Jason-1 data [Collard, 2005]
Rain Flag	Derived from comparisons to thresholds of the radiometer-derived integrated liquid water content and of the difference between the measured and the expected Ku-band backscatter coefficient
Ice Flag	Derived from comparison of the model wet tropospheric correction to a dual-frequency wet tropospheric correction retrieved from radiometer brightness temperatures, with a default value issued from a climatology table

Table 13. Models and standards (Jason-3 Product Version “F”)

### 3.2. Models and Editing on Version “f” Products

#### 3.2.1. Orbit models

Jason-2 orbit standards are based on version “POE-F” orbit model. Its characteristics are summarized below. Previous standard used on Jason-2 mission (POE-E) is also recalled:

	POE-E	POE-F
--	-------	-------



<p><b>Gravity model</b></p>	<p>EIGEN-GRGS.RL03-v2.MEAN-FIELD</p> <p>Non-tidal TVG: one annual, one semi-annual, one bias and one drift terms for each year up to deg/ord 80; C21/S21 modeled according to IERS2010 conventions</p> <p>Solid Earth tides: from IERS2003 conventions</p> <p>Ocean tides: FES2012</p> <p>Oceanic/atmospheric gravity: 6hr NCEP pressure fields (70x70) + tides from Biancale-Bode model</p> <p>Pole tide: solid Earth and ocean from IERS2010 conventions</p> <p>Third bodies: Sun, Moon, Venus, Mars and Jupiter</p>	<p>EIGEN-GRGS.RL04-v1.MEAN-FIELD</p> <p>Non-tidal TVG: one annual, one semi-annual, one bias and one drift terms for each year up to <b>deg/ord 90; C21/S21 non modified</b></p> <p>Unchanged</p> <p>Ocean tides: <b>FES2014</b></p> <p>Oceanic/atmospheric gravity: <b>3hr dealiasing products from GFZ AOD1B RL06</b></p> <p>Unchanged</p> <p>Unchanged</p>
<p><b>Surface forces</b></p>	<p>Radiation pressure model: calibrated semi-empirical solar radiation pressure model</p> <p>Earth radiation: Knocke-Ries albedo and IR satellite model</p> <p>Atmospheric density model: DTM-13 for Jason satellites, HY-2A, and MSIS-86 for other satellites</p>	<p>Unchanged</p> <p>Unchanged</p> <p>Atmospheric density model: DTM-13 for Jason satellites, HY-2A, and <b>MSIS-00 for other satellites</b></p>
<p><b>Estimated dynamical parameters</b></p>	<p>Stochastic solutions</p>	<p>Unchanged</p>
<p><b>Satellite reference</b></p>	<p>Mass and center of gravity: post-launch values + variations generated by Control Center</p> <p>Attitude model:</p> <p>For Jason satellites: quaternions and solar panel orientation from control center, completed by nominal yaw steering law when necessary</p> <p>Other satellites: nominal attitude law</p>	<p>Unchanged</p> <p><b>Refined nominal attitude laws</b></p>
<p><b>Displacement of reference points</b></p>	<p>Earth tides: IERS2003 conventions</p> <p>Ocean loading: FES2012</p> <p>Pole tide: solid earth pole tides and ocean pole tides (Desai, 2002),</p>	<p>Unchanged</p> <p>Ocean loading: <b>FES2014</b></p> <p>Pole tide: solid earth pole tides and ocean pole tides (Desai, 2002), <b>new linear mean pole model</b></p>



	<p>cubic+linear mean pole model from IERS2010</p> <p>S1-S2 atmospheric pressure loading, implementation of Ray &amp; Ponte (2003) by van Dam</p> <p>Reference GPS constellation: JPL solution - fully consistent with IGS08</p>	<p>Unchanged</p> <p>Reference GPS constellation: <b>GRG solution - fully consistent with IGS14</b></p>
<b>Geocenter variations</b>	<p>Tidal: ocean loading and S1-S2 atmospheric pressure loading</p> <p>Non-tidal: seasonal model from J. Ries, applied to DORIS/SLR stations</p>	<p>Unchanged</p> <p>Non-tidal: <b>full non-tidal model (semi-annual, annual, inter-annual) derived from DORIS data and the OSTM/Jason-2 satellite, applied to DORIS/SLR stations and GPS satellites</b></p>
<b>Terrestrial Reference Frame</b>	<p>Extended ITRF2008 (SLRF/ITRF2008, DPOD2008, IGS08)</p>	<p><b>Extended ITRF2014 (SLRF/ITRF2014, DPOD2014, IGS14)</b></p>
<b>Earth orientation</b>	<p>Consistent with IERS2010 conventions and ITRF2008</p>	<p>Consistent with IERS2010 conventions and <b>ITRF2014</b></p>
<b>Propagations delays</b>	<p>SLR troposphere correction: Mendes-Pavlis</p> <p>SLR range correction: constant 5.0 cm range correction for Envisat, elevation dependent range correction for Jason</p> <p>DORIS troposphere correction: GPT/GMF model</p> <p>DORIS beacons phase center correction</p> <p>GPS PCO/PCV (emitter and receiver) consistent with constellation orbits and clocks (IGS08 ANTEX), pre-launch GPS receiver phase map</p> <p>GPS: phase wind-up correction</p>	<p>Unchanged</p> <p>SLR range correction: <b>geometrical models for all satellites</b></p> <p>DORIS troposphere correction: <b>GPT2/VMF1 model</b></p> <p>Unchanged</p> <p>GPS PCO/PCV (emitter and receiver) consistent with constellation orbits and clocks (<b>IGS14 ANTEX</b>), <b>in-flight adjusted GPS receiver phase map</b></p> <p>Unchanged</p>
<b>Estimated measurement parameters</b>	<p>DORIS: one frequency bias per pass, one troposphere zenith bias per pass</p> <p>SLR: Reference used to evaluate orbit precision and stability</p> <p>GPS: floating ambiguity per pass, receiver clock adjusted per epoch</p>	<p>DORIS: one frequency bias <b>and drift (for "SAA stations")</b> per pass, one troposphere zenith bias per pass, <b>horizontal tropospheric gradients per arc</b></p> <p>Unchanged</p> <p>GPS: <b>fixed ambiguity (when possible)</b> per pass, receiver clock adjusted per epoch</p>
<b>Tracking Data corrections</b>	<p>Jason-1 Doris data: updated South Atlantic Anomaly model (J.-M. Lemoine)</p>	<p>Unchanged</p>



	<p>et al.) applied before and after DORIS instrument change</p> <p>DORIS time-tagging bias for Envisat and Jason aligned with SLR before and after instrument change</p>	<p>Unchanged</p>
<b>Doris Weight</b>	<p>1.5 mm/s (1.5 cm over 10 sec)</p> <p>For Jason-1, SAA DORIS beacons weight is divided by 10 before DORIS instrument change</p>	<p>Process data down to as low elevation angles as possible (from 10° to 5° elevation cut-off angle) with a consistent down-weighting law</p> <p>Unchanged</p>
<b>SLR Weight</b>	<p>15 cm</p> <p>Reference used to evaluate orbit precision and stability</p>	<p>Unchanged</p>
<b>GPS Weight</b>	<p>2 cm (phase) / 2 m (code)</p>	<p>Unchanged</p>

Table 14. POE-E-D/POE-F orbit standard

### 3.2.2. Mean Sea Surface

#### 3.2.2.1. MSS\_CNES-CLS15

The MSS\_CNES-CLS15 model is computed from 16 years of satellite altimetry data from a variety of missions. Its main characteristics are the following :

<b>Name</b>	MSS_CNES-CLS15
<b>Reference ellipsoid</b>	T/P
<b>Referencing time period</b>	1993-2013 (20 years)
<b>Spatial coverage</b>	Global (80°S to 84°N) - Oceanwide where altimetric data are available. Undefined on continents.
<b>Spatial resolution</b>	Regular grid with a 1/60° (1 minutes) spacing (i.e. ~2 km)
<b>Grid</b>	21600 points in longitude / 9841 points in latitude
<b>MSS determination technique</b>	Local least square collocation method on a 3' grid where altimetric data in a 200-km radius are selected. Estimation on a 1' grid based on SSH-Filtered MSS values (remove/restore technique to recover the full signal). The inverse method uses local anisotropic covariance functions which improve the shortest wavelengths.
<b>Estimation error level</b>	YES (in cm) - The Optimal Interpolation method provides a calibrated formal error
<b>Altimetric dataset</b>	T/P-J1-J2: 20 years mean profile (first orbit), T/P tandem & J1 tandem: 3.7 years profile GFO: 7 years mean profile ERS-2/EnviSat: 15 years mean profile, 1 year ERS-1 (geodetic phase) J1 & Cryosat-2: geodetic phase

Table 15 : MSS\_CNES-CLS15 model characteristics

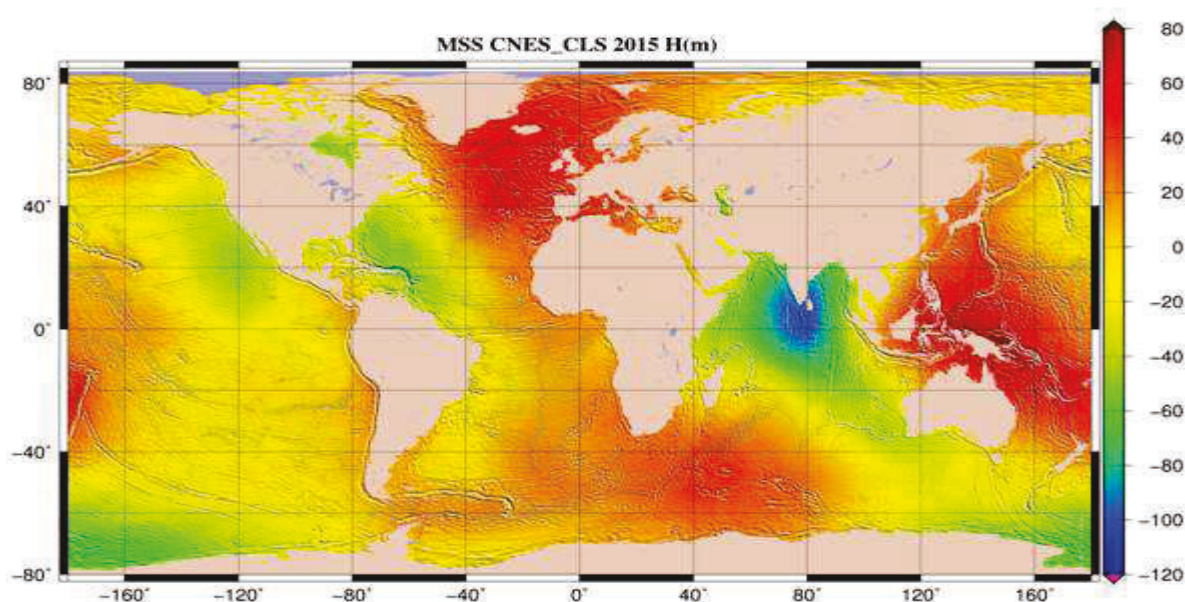


Figure 12 : Mean Sea Surface MSS\_CNES-CLS15.

Refer to <http://www.aviso.altimetry.fr/en/data/products/auxiliary-products/mss/index.html> for more details on this model.



---

### 3.2.2.2. MSS\_DTU-2018

Refer to :

Andersen, O., Knudsen, P., & Stenseng, L. (2018). A New DTU18 MSS Mean Sea Surface - Improvement from SAR Altimetry. 172. Abstract from 25 years of progress in radar altimetry symposium, Portugal.

[ftp://ftp.space.dtu.dk/pub/DTU18/1\\_MIN/](ftp://ftp.space.dtu.dk/pub/DTU18/1_MIN/)

### 3.2.3. Mean Dynamic Topography

The MDT\_CNES-CLS18 model is computed from satellite altimetry data from a variety of missions. Its main characteristics are the following :

<b>Name</b>	MDT_CNES-CLS18
<b>Referencing time period</b>	1993-2012 (20 years)
<b>Domain</b>	Global - no Black Sea - no dedicated processing in the Arctic - the Med Sea come from the regional SOCIB MDT (Rio et al., 2014)
<b>Spatial resolution</b>	Regular grid with a 1/8°
<b>Grid</b>	2880 points in longitudes / 1440 points in latitude
<b>MDT determination technique</b>	Reference of the altimeter Sea Level Anomalies, computed relative to a 20 years (1993-2012) mean profile, in order to obtain absolute measurements of the ocean dynamic topography. Combined product based on GRACE and GOCE gravimetric data, altimetry and in situ data (hydrologic and drifters data)

**Table 16 :** MDT\_CNES-CLS18 model characteristics

This sea surface height (mean sea surface height above geoid) corresponds to mean geostrophic currents and its changes.

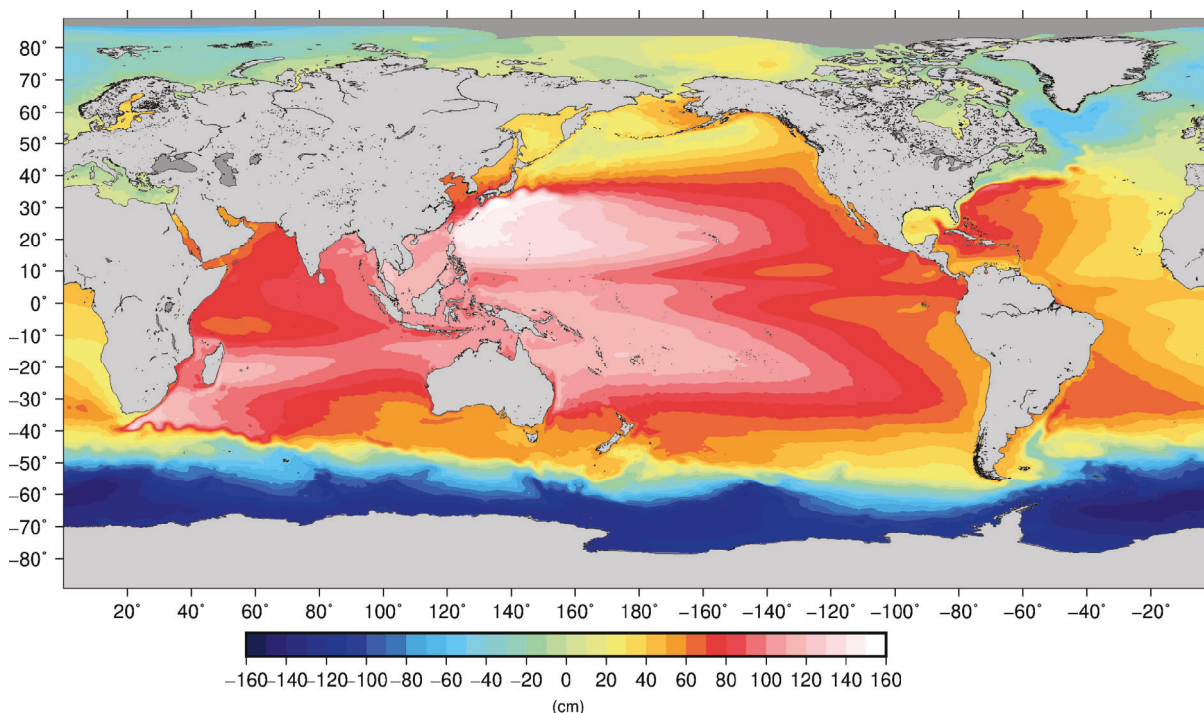


**Figure 13 :** Mean Dynamic Topography MDT\_CNES-CLS18

Refer to <http://www.aviso.altimetry.fr/en/data/products/auxiliary-products/mdt/index.html> for more details on this model.

### 3.2.4. Geoid

Jason-2 GDRs use the EGM2008 geopotential to compute the geoid [Pavlis *et al.*, 2012].

EGM2008 is a spherical harmonic model of the Earth's gravitational potential, developed by a least squares combination of the ITG-GRACE03S gravitational model and its associated error covariance matrix. This grid was formed by merging terrestrial, altimetry-derived, and airborne gravity data.

The EGM2008 gravitational model has been used to calculate point values of geoid undulation on a 5 x 5 minute grid that spans the latitude range +90.0 deg. to -90.0 deg. The EGM2008 model is complete to spherical harmonic degree and order 2159 and contains additional coefficients up to degree 2190 and order 2159.

It has been corrected so as to refer to the reference ellipsoid (WGS84) and to add the permanent tide (zero frequency) [Rapp *et al.*, 1991].

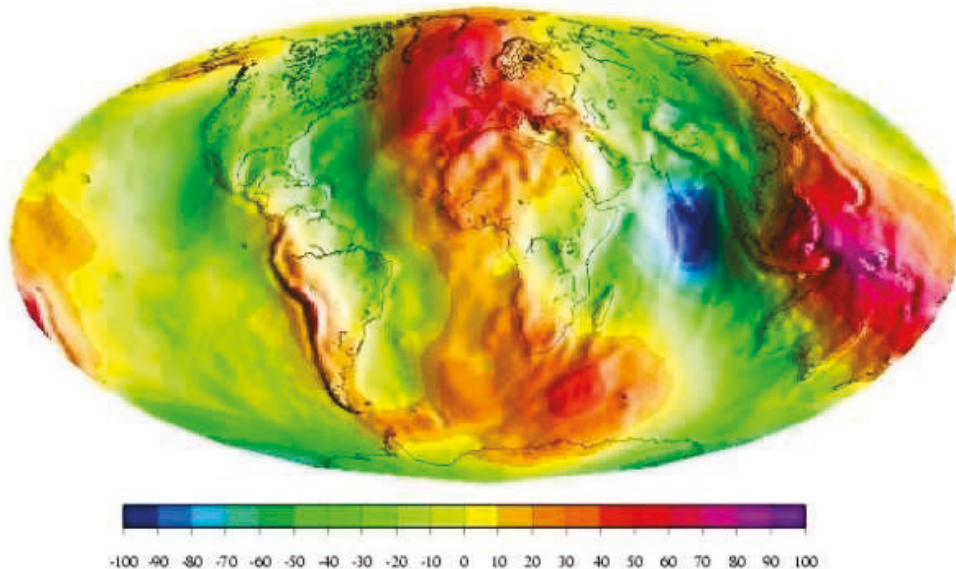


Figure 14 : EGM2008 geoid

More information on EGM08 can be found at <http://onlinelibrary.wiley.com/doi/10.1029/2011JB008916/full>

### 3.2.5. Bathymetry

The value of this parameter is determined from the ACE2 (Altimeter Corrected Elevations) digital elevation model at 30" resolution [Berry, P.A.M.; Smith,R.; Benveniste,J., 2008].

ACE2 digital elevation model has been created by synergistically merging the SRTM dataset with Satellite Radar Altimetry within the region bounded by  $\pm 60N$ .

Over the areas lying outside the SRTMs latitude limits other sources have been used such as including GLOBE and the original ACE DEM, together with new matrices derived from reprocessing the ERS1 Geodetic Mission dataset with an enhanced retracking system, and the inclusion of data from other satellites.

### 3.2.6. Ocean Tides

The two geocentric tide values provided on the Jason-3 (O)(I)GDR, `ocean_tide_got` and `ocean_tide_fes` are computed with diurnal and semidiurnal ocean and load tide values predicted by the GOT4.10c and FES2014b models, respectively.

Both geocentric ocean tide fields (`ocean_tide_got` and `ocean_tide_fes`) include the load tides from `load_tide_got` and `load_tide_fes` fields respectively, and the equilibrium long-period ocean tide (`ocean_tide_eq`). The GOT4.10c model includes only one non-linear wave (M4), and FES2014b includes several non-linear waves: M4, M6, M8, MKS2, MN4, MS4, MSf, N4, S4.

Both models are interpolated to provide the geocentric ocean and load tides at the location of the altimeter measurement, and an interpolation quality flag is provided on the (O)(I)GDRs to indicate the quality of this interpolation (see `ocean_tide_fes_interp_qual` and `ocean_tide_got_interp_qual` ).



## 3.2.6.1. GOT4.10c Ocean Tide Model

Solution GOT4.10c [Ray, 2013; Ray, personal communication], is the last version of GOT models developed by R. Ray.

This model is different from previous version GOT4.8 as it is now based on Jason-1 and Jason-2 data, ERS-1 and ERS-2 and GFO.

None T/P data has been used in this solution.

The solution consists of independent near-global estimates of 10 tidal constituents (Q1, O1, P1, S1, K1, N2, M2, S2, K2, M4) for both the oceanic and the loading tide components. An a priori model was used that consisted of the hydrodynamic model FES 2004 [Lyard et al. 2006] and several other local hydrodynamic models.

Note that GOT4.10c model uses the new tidal geocenter correction proposed by Shailen and Ray (2014). Moreover the dry-tropospheric correction used for the Jason satellites never had the S2 air-tide error that the original T/P data had.

GOT4.10c solution does not use the Cg correction, as it is a T/P correction.

GOT4.10c solution is provided on a 0.5° grid; moreover the ocean tide grids have been extrapolated on one pixel over coasts and ocean tide values are set to zero on lakes and enclosed-seas.

## 3.2.6.2. FES2014b Ocean Tide Model

FES2014 is the last version of the FES (Finite Element Solution) tide model developed in 2014-2016. It is an improved version of the FES2012 model, which was a fully revised version of the global hydrodynamic tide solutions initiated by the work of Christian Le Provost in the early nineties. This new FES2014 model has been developed, implemented and validated by the LEGOS, NOVELTIS and CLS, within a CNES funded project.

FES2014 takes advantage of longer altimeter time series and better altimeter standards, improved modelling and data assimilation techniques, a more accurate ocean bathymetry and a refined mesh in most of shallow water regions. Special efforts have been dedicated to address the major non-linear tides issue and to the determination of accurate tidal currents.

FES2014 is based on the resolution of the tidal barotropic equations (T-UGO model) in a spectral configuration.

A new global finite element grid (~2.9 million nodes, 50% more than FES2012) is used and model physic has been improved, leading to a nearly twice more accurate 'free' solution (independent of in situ and remote-sensing data) than the previous FES2012 version. Then the accuracy of this 'free' solution was improved by assimilating some long-term altimetry data (Topex/ Poseidon, Jason-1, Jason-2, TPN-J1N, and ERS-1 - ERS-2 - ENVISAT) and tidal gauges through an improved representer assimilation method.

A preliminary version, noted FES2014a, has been produced in 2015 based on GOT4v8ac loading tide. Then new tide loading effects have been computed using FES2014a oceanic tide (J.P. Boy, Univ. Strasbourg). These FES2014a tide loading effects have been used to produce the final model version noted FES2014b, which is used in Jason-3 GDR-F:

FES2014b geocentric (elastic) tide = FES2014b oceanic tide + FES2014a loading tide.

Final FES2014b solution shows strong improvement compared to FES2012 and GOT4V10, particularly in coastal and shelf regions and also in some deep ocean areas and in the Arctic region.

34 tidal constituents are available for both the oceanic tide and the loading tide components : 2N2, EPS2, J1, K1, K2, L2, La2, M2, M3, M4, M6, M8, Mf, MKS2, Mm, MN4, MS4, MSf, MSqm, Mtm, Mu2, N2, N4, Nu2, O1, P1, Q1, R2, S1, S2, S4, Sa, Ssa, T2.

FES2014b solution is provided on a 1/16° grid; moreover the ocean tide grids have been extrapolated on ten pixels over coasts and ocean tide values are set to zero on lakes and enclosed-seas.

See "<http://www.aviso.altimetry.fr/en/data/products/auxiliary-products/global-tide-fes.html>" for more information.



### 3.2.7. Sea Surface Height Bias model

The Sea State Bias (SSB) can be defined as the difference between the apparent sea level as “seen” by the altimeter and the actual mean sea level. It is composed of: the Electromagnetic bias (EMB), and skewness and tracker biases that affect the accuracy of altimeter measurements and are all dependent on SWH. The EMB (main contributor) results from the fact that the radar senses an average sea surface lower than the true average sea surface, due to amplification from wave troughs. This bias can be expressed as a percentage of SWH, with the percentage being a complex function of the sea-surface slope and elevation statistical distribution.

Consolidated empirical Jason-2 SSB solutions have been developed from the Jason-3 measurements [Tran 2019]. The standard 2D version is a function of SWH and altimeter wind speed while the improved 3D version uses additionally a mean wave period estimate from wave model to better describe the local wave conditions.

### 3.2.8. Wave model

Jason-2 GDRs use Meteo France MFWAM model WAVERYS as wave model to compute the 3D SSB. This value is reported in the product (variable mean\_wave\_period\_t02) , so is the mean wave direction (variable mean\_wave\_direction)

### 3.2.9. Surface Classification Map

Jason-2 GDRs provide a 7 classes Surface Classification Flag (surface\_classification\_flag).

GDR-D	GDR-F
surface_type (4 classes)	surface_classification_flag (7 classes)
0: ocean	0:open_ocean
1: lake_enclosed_sea	1:land
2: ice	2:continental_water
3: land	3:aquatic_vegetation
	4:continental_ice_snow
	5:floating_ice
	6:salted_basin

The map used for GDR-F Surface Classification consists in the combination of three data sources :

- GMT surface mask developed by Noveltis for the generation of the Jason-2 MNT (also including water body outlines from the LEGOS database)
- GLOBCOVER LC V2.0
- MODIS Mosaic of Antarctica from NSIDC

### 3.2.10. Coastal Distance & Angle of Approach to Coast

Coastal distance computation and angle of approach to coast (see distance\_to\_coast and angle\_of\_approach\_to\_coast) determination is based on GSHHG\_v2.3.7 model.

### 3.2.11. Global Slope Correction

Jason-2 GDRs use [Sandwell 3103] to compute the range reduction caused by the slope of the geoid relative to the ellipsoid.



---

This correction is NOT included in the ssha, and shall not be used with the mean sea surface (mean\_sea\_surface\_cnescls or mean\_sea\_surface\_dtu) provided in the product.

### 3.2.12. Sea Ice Concentration

Jason-2 GDRs use Eumetsat OSISAF “ice conc” to determine the sea ice concentration (variable sea\_ice\_concentration).

- For data before 31 Dec 2015, version used is OSI-450 CDR-ease
- For data from 1 Jan 2016 onwards, version used is OSI-430-b ICDR-ease



# OSTM/Jason-2 Products Handbook

Iss :2.0- date : Apr 15th , 2025



42





## 4. Using the (O)(I)GDR data

### 4.1. Overview

This section gives the reader a guide to the use of the OSTM/Jason-2 (O)(I)GDR data. While this handbook tries to be correct and complete, note that nothing can replace the information to be gained at conferences and other meetings from those using these data. The reader must proceed with caution and at his or her own risk. Further information is also available on the web servers provided in Annex C, please direct questions and comments to the contacts given there.

The instruments on OSTM/Jason-2 make direct observations of the following quantities: altimeter range, ocean significant wave height, ocean radar backscatter cross-section (a measure of wind speed), ionospheric electron content in the nadir direction, tropospheric water content, and position relative to the GPS satellite constellation. Ground based laser station and DORIS station measurements of the satellite location and speeds are used in precision orbit determination (POD). The DORIS stations also measure the ionospheric electron content along the line of sight to the satellite. All of these measurements are useful in themselves, but they are made primarily to derive the sea surface height with the highest possible accuracy. Such a computation also needs external data (not collected aboard OSTM/Jason-2), e.g., atmospheric pressure, etc. In addition, instrument health and calibration data are collected onboard and used to make corrections to the main measurements and to monitor the instrument stability in the long term.

This (O)(I)GDR contains all relevant corrections needed to calculate the sea surface height. For the other "geophysical variables" in the (O)(I)GDR: ocean significant wave height, tropospheric water content, ionospheric electron content (derived by a simple formula), and wind speed, the needed instrument and atmospheric corrections have already been applied.

The following sections explain the rationale for how the corrections should be applied.

### 4.2. Data Editing criteria recommendation

The following editing criteria are a recommended guideline for finding good records from the (O)(I)GDR to calculate the sea level anomaly from the Ku band range. The user should review these criteria before using them and may wish to modify them!

First, check the following conditions to retain only ocean data and remove any bad, missing, or flagged data:

Parameter	Value	Meaning
surface_type	0	Open oceans or semi-enclosed seas
ice_flag	0	No ice

Table 17 : Recommended editing criteria

Then, filter the data as follows to retain only the most valid data :

Parameter	Validity conditions
range_numval_ku	$10 \leq x$
range_rms_ku	$0 \leq x \text{ (mm)} \leq 200$
altitude - range_ku	$-130\ 000 \leq x \text{ (mm)} \leq 100\ 000$
model_dry_tropo_corr	$-2\ 500 \leq x \text{ (mm)} \leq -1\ 900$
rad_wet_tropo_corr	$-500 \leq x \text{ (mm)} \leq -1$
iono_corr_alt_ku	$-400 \leq x \text{ (mm)} \leq 40$
sea_state_bias_ku	$-500 \leq x \text{ (mm)} \leq 0$
ocean_tide_sol1	$-5\ 000 \leq x \text{ (mm)} \leq 5\ 000$
solid_earth_tide	$-1\ 000 \leq x \text{ (mm)} \leq 1\ 000$
pole_tide	$-150 \leq x \text{ (mm)} \leq 150$
swh_ku	$0 \leq x \text{ (mm)} \leq 11\ 000$
sig0_ku	$7 \leq x \text{ (dB)} \leq 30$



wind_speed_alt	$-0 \leq x \text{ (m/s)} \leq 30$
off_nadir_angle_wf_ku	$-0.2 \leq x \text{ (deg}^2\text{)} \leq 0.64$
sig0_rms_ku	$x \text{ (dB)} \leq 1$
sig0_numval_ku	$10 < x$

Table 18 : Recommended filtering criteria

To restrict studies to deep water, apply a limit, e.g., water depth of 1000m or greater, using the bathymetry parameter (ocean depth in meters.)

### 4.3. Typical computation from altimetry data

In this section references are made to specific (O)(I)GDR parameters by name using the name of the variable as described in the NetCDF data sets.

In addition with the MLE-4 retracking parameters, MLE-3 retracker parameters are also included in the Jason-2 products since the GDR-D version. Altimeter parameters (e.g. Range, swh, sigma0, etc) and related geophysical parameters (e.g. Ionosphere correction, sea state bias correction, wind speed, etc) named without the "mle3" extension are derived from MLE-4 retracking, while those with the "mle3" extension are derived from MLE-3 retracking

Most users are advised to use the MLE-4 altimeter parameters for typical scientific applications. The MLE-3 Ku-band parameters are provided for the convenience of specialized studies on the calibration and validation of the mission and impact of altimeter retracking.

#### WARNING

Default values are given to data when computed values are not available (See section 1.1) so you must screen parameters to avoid using those with default values. Also you must check flag values. The related flags are given in the description of each variable (See section 1.1) although some discussion of flags appears in this section.

#### 4.3.1. Corrected Altimeter Range

The main data of the (O)(I)GDR are the altimeter ranges. The (O)(I)GDR provides ranges measured at Ku band (ku/range\_ocean, resp. ku/range\_ocean\_mle3 for MLE3, resp. ku/range\_adaptive for Adaptive)) and C band (c/range\_ocean). The Ku band range is used for most applications. The given ranges are corrected for instrumental effects. These corrections are separately reported for each of the Ku ((ku/range\_cor\_ocean\_net\_instr, resp. ku/range\_cor\_ocean\_mle3\_net\_instr for MLE3) and C band ranges (c/range\_cor\_ocean\_net\_instr).

The given ranges must be corrected for path delay in the atmosphere through which the radar pulse passes and the nature of the reflecting sea surface. All range corrections are defined and they should be ADDED to the range. The corrected (Ku band) range is given by

Corrected Range = Range	+ Wet Troposphere Correction
	+ Dry Troposphere Correction
	+ Ionosphere Correction
	+ Sea State Bias Correction

#### Wet Troposphere Correction :

Use AMR correction (rad\_wet\_tropo\_cor).

#### Dry Troposphere Correction :

Use model correction (model\_dry\_tropo\_cor\_zero\_altitude).

#### Ionosphere Correction :

Use MLE4 altimeter ionosphere filtered correction (iono\_cor\_alt\_filtered) to correct Ku range issued from MLE4 retracking (ku/range\_ocean).



Use MLE3 altimeter ionospheric filtered correction (iono\_cor\_alt\_filtered\_mle3) to correct Ku range issued from MLE3 retracking (ku/range\_ocean\_mle3).

Use Adaptive altimeter ionospheric filtered correction (iono\_cor\_alt\_filtered\_adaptive) to correct Ku range issued from Adaptive retracking (ku/range\_adaptive). IMPORTANT: See Section 1.1.1 "Smoothing the Ionosphere Correction".

**Sea State Bias Correction :**

Use MLE4 sea state bias correction (ku/sea\_state\_bias) to correct Ku range issued from MLE4 retracking (ku/range\_ocean).

Use MLE3 sea state bias correction (ku/sea\_state\_bias\_mle3) to correct Ku range issued from MLE3 retracking (ku/range\_ocean\_mle3).

Use Adaptive sea state bias correction (sea\_state\_bias\_adaptive) to correct Ku range issued from Adaptive retracking (ku/range\_adaptive).

Use improved version (sea\_state\_bias\_3d\_mp2) for fine regional studies

**4.3.2. NOTE: The ionosphere and sea state bias corrections are both frequency dependent. Therefore Ku band corrections should only be applied to Ku band ranges, and C band corrections should only be applied to C band ranges. Section 4.2.4 explains how the C band ionosphere correction can be derived from the Ku band ionosphere correction (iono\_cor\_alt, resp. iono\_cor\_alt\_mle3 for MLE3), while the C band sea state bias correction is provided as c/sea\_state\_bias (resp. c/sea\_state\_bias\_mle3 for MLE3). Sea Surface Height and Sea Level Anomaly**

Sea surface height (SSH) is the height of the sea surface above the reference ellipsoid. It is calculated by subtracting the corrected range from the Altitude:

$$\text{Sea Surface Height} = \text{Altitude} - \text{Corrected Range}$$

The sea level anomaly (SLA), also referred to as Residual Sea Surface, is defined here as the sea surface height minus the mean sea surface and minus known geophysical effects, namely tidal and inverse barometer. It is given by:

$$\begin{aligned} \text{Sea Level Anomaly} = & \text{Sea Surface Height} - \text{Mean Sea Surface} \\ & - \text{Solid Earth Tide Height} \\ & - \text{Geocentric Ocean Tide Height} \\ & - \text{Non Equilibrium Long Period Tide Height} \\ & - \text{Internal Tide Height} \\ & - \text{Pole Tide Height} \\ & - \text{Dynamic Atmospheric Correction} \end{aligned}$$

The SLA contains information about:

- Real changes in ocean topography related to ocean currents
- Dynamic response to atmospheric pressure
- Differences between tides and the tide models
- Differences between the mean sea surface model and the true mean sea surface at the OSTM/Jason-2 location
- Unmodeled or mismodeled measurement effects (skewness, sea state bias, altimeter errors, tropospheric corrections, ionospheric correction, etc.)
- Orbit errors

There is naturally also random measurement noise. Understanding the first four items as a function of space and time is the purpose of OSTM/Jason-2.

**Altitude :**

Orbit altitude (see parameter altitude)



**Corrected Range :**

See section 4.3.1.

**Tide effects** (solid earth tide height, geocentric ocean tide height, pole tide height, Non Equilibrium long period t height, internal tide height) :

See sections 4.3.2.1 and 5.10.

**Dynamic Atmospheric Correction:**

Use dac (see also section 5.11).

**Mean Sea Surface :**

See sections 4.3.2.2 and 5.4.

**4.3.2.1. Tide Effects**

The total tide effect on the sea surface height is the sum of three values from the GDR:

$$\begin{aligned} \text{Tide Effect} &= \text{Geocentric Ocean Tide} \\ &+ \text{Non Equilibrium Long Period} \\ &+ \text{Solid Earth Tide} \\ &+ \text{Pole Tide} \\ &+ \text{Internal Tide} \end{aligned}$$

(See also section 5.10 and subsections)

**Geocentric Ocean Tide :**

The geocentric ocean tide provided on the GDR is actually the sum total of the ocean tide effect and the self-attraction and loading tide effect.

$$\text{Geocentric Ocean Tide} = \text{Ocean Tide} + \text{Load Tide}$$

The (O)(I)GDR provides a choice of two geocentric ocean tide values, `ocean_tide_fes` and `ocean_tide_got`. Each uses a different model for the sum of the ocean tide and loading tide heights for high frequencies (diurnal, semi-diurnal and non-linear tides with higher frequencies), but both include an equilibrium representation of the long-period ocean tides at all long-periods except for the zero frequency (permanent tide) term which is not included. Note that the (O)(I)GDR also explicitly provides the loading tide height from each of the two models that are used to determine the two geocentric ocean tide values, `load_tide_fes`, `load_tide_got`, so the pure ocean tide can be determined by subtracting the load tide value from the geocentric ocean tide value. Obviously, the geocentric ocean tide values and loading tide values should added simultaneously, since the loading tide height would be modeled twice.

**Non Equilibrium long-period Tide :**

Use `ocean_tide_non_eq`

$$\text{Geocentric Ocean Tide} = \text{Ocean Tide} + \text{Load Tide} + \text{Non Equilibrium Long-Period Tide}$$

Adding the field `tide_neq_lp` to the geocentric ocean tide, allows computing a more complete geocentric ocean tide signal including the dynamic ocean response and the corresponding SAL effect for 6 long period tidal frequencies.

**Solid Earth Tide :**

Use `solid_earth_tide`

NOTE: Zero frequency (permanent tide) term is not included in this parameter.

**Pole Tide :**



Use pole\_tide

The tide values all have the same sign/sense in that positive numbers indicate that the surface is farther from the center of the Earth.

**Internal Tide :**

Use internal\_tide

The (O)(I)GDR provides one internal tide value, computed from Zaron (2019) model. It models the internal tides surface signatures which remain coherent with the four main barotropic tide frequencies.

### 4.3.2.2. Geophysical Surface - Mean Sea Surface or Geoid

The geophysical fields Geoid (geoid) - actually geoid undulation, but called simply geoid - and Mean Sea Surface (mean\_sea\_surface\_cnescls and mean\_sea\_surface\_dtu) are distances above the reference ellipsoid, as is the Sea Surface Height. These values are for the location indicated by latitude and longitude. If the values of these fields are needed at a different location within the current frame, along-track interpolation may be done using the high rate (20/second) range and altitude values.

As the geoid is derived from the mean sea surface, the latter is the better-known quantity. The residual surface with respect to the geoid is sometimes called the "dynamic topography" of the ocean surface.

See also discussions of mean sea surface and geoid in sections 5.3 and 5.4.

### 4.3.3. Mean Sea Surface and Adjustment of the Cross Track Gradient

In order to study sea level changes between two dates, it is necessary to difference sea surface heights from different cycles at the exact same latitude-longitude, so that the not well-known time-invariant geoid cancels out. However, the (O)(I)GDR samples are not given at the same latitude-longitude on different cycles. They are given approximately every 1 sec along the pass (about 6 km, the time difference and distance vary slightly with satellite height above the surface), and the satellite ground track is allowed to drift by  $\pm 1$  km. This introduces a problem: on different cycles the satellite will sample a different geoid profile. This effect is the so-called cross-track geoid gradient, and *Brenner and Koblinsky* [1990] estimated it at about 2 cm/km over most of the ocean, larger over continental slopes, reaching 20 cm/km at trenches. Even if the passes repeated exactly, one would have to interpolate along the pass (say, to a fixed set of latitudes) because a 3 km mismatch in along pass position would cause approximately a 6 cm difference in the geoid, which would mistakenly be interpreted as a change in oceanographic conditions.

Both problems are simultaneously solved if the quantity one interpolates along a given pass is the difference

Residual Height - Mean Sea Surface

Then the real geoid changes across the track are automatically accounted for (to the extent the MSS model is close to the true geoid) because the MSS is spatially interpolated to the actual satellite latitude-longitude in the (O)(I)GDR. The residual height term above is the residual sea surface height after applying all the tidal, atmospheric and ionospheric corrections, etc. Otherwise, those need to be interpolated separately.

One possible approach is to interpolate along track to a set of common points, a "reference" track. The reference could be:

- An actual pass with maximum data and/or minimum gaps, or
- A specially constructed fixed track (see below)

The procedure is the following:



- For each common point, find neighboring points in the pass of interest (POI).
- In the POI, interpolate along track to the common point, using longitude as the independent variable, for each quantity of interest - sea surface height (see above), mean sea surface, geoid, tides, etc.
- As stated above, the quantity to compare at each common point is :

$$\Delta\text{SSH} = \text{Interpolated POI SSH} - \text{Interpolated POI MSS}$$

- Other geophysical corrections must be applied to dSSH, depending on the type of investigation

The geoid model in the (O)(I)GDR could substitute the MSS model, but its use will result in reduced accuracy in the interpolation because the resolution of the geoid undulation is lower than that of the MSS.

Desirable features of a fixed reference track include:

- Equal spacing of points (good for FFT)
- Independent variable = (point longitude - pass equator crossing longitude)
- Equator is a point (simplifies calculation)
- Point density similar to original data density

With these specifications, it is possible to make only two fixed tracks, one ascending and one descending, which will serve for all passes. The template pass is then shifted by the equator crossing longitude (global attribute of the product, see 1.1) of each pass. Recall that the equator longitude is from a predicted orbit (not updated during GDR processing). Improved accuracy can be obtained by interpolating in the latitude, longitude values. When one interpolates to the reference track, it is good practice to check that the interpolated latitude from the data records used is close to the latitude on the reference track.

#### 4.3.4. Total Electron Content from Ionosphere Correction

To calculate Ionospheric Total Electron Content, TEC, use the following formula:

$$\text{Ionospheric Total Electron Content} = \frac{dR * f^2}{40.3}$$

Where :

- Ionospheric Total Electron Content is in electrons/m<sup>2</sup>
- dR = Ku band ionospheric range correction from the (O)(I)GDR in meters (iono\_corr\_alt\_ku, resp. iono\_corr\_alt\_ku\_mle3 for MLE3)
- f = frequency in Hz (13.575 GHz for the Ku band)

Note that the TEC could then be converted to a C band ionosphere range correction using the same formula above, but with the C band frequency of 5.3 GHz.

#### 4.3.5. Range Compression

Each 1Hz frame of the Poseidon-3B Ku (data01/ku/range\_ocean, resp. data01/ku/range\_ocean\_mle3 for MLE3) and C band range measurements (data01/c/range\_ocean) are derived from the linear regression of the respective valid 20 Hz range measurements (data\_20/ku/range\_ocean, resp. data\_20/ku/range\_ocean\_mle3 for MLE3, data\_20/ku/range\_adaptive for Adaptive and data\_20/c/range\_ocean).

An iterative outlier detection scheme is adopted in this linear regression and the resulting 20 Hz measurements are identified by setting the corresponding parameter (range\_ocean\_compression\_qual, resp. range\_ocean\_mle3\_compression\_qual, range\_adaptive\_compression\_qual) to 1. Measurements not considered as outliers have the parameter set to 0.



---

The number of valid 20 Hz measurements that are used to derive each of the 1 Hz measurements is provided on the (O)(I)GDRs (ku/range\_ocean\_numval, resp. ku/range\_ocean\_mle3\_numval for MLE3, resp. ku/range\_adaptive\_numval for Adaptive, and c/range\_ocean\_numval ), as are the root-mean-square of the differences between the valid 20 Hz measurements and the derived 1 Hz measurement (ku/range\_ocean\_rms, resp. ku/range\_ocean\_mle3\_rms for MLE3, resp. ku/range\_adaptive\_rms for Adaptive and ku/range\_ocean\_rms).



## 5. Altimetric data

This section presents a short discussion of the main quantities on the (O)(I)GDR.

An excellent overview of the theoretical and practical effects of radar altimetry is the “Satellite Altimetry” Chapter by *Chelton et al* [2001].

### 5.1. Precise Orbits

CNES has the responsibility for producing the orbit ephemerides for the OSTM/Jason-2 data products. The OSTM/Jason-2 OGDRs provide a navigator orbit that has radial accuracies better than 5 cm (RMS), the OSTM/Jason-2 IGDRs provide a preliminary orbit that has radial accuracies better than 2.5 cm (RMS), while the GDRs provide a precise orbit that has radial accuracies better than 1.5 cm (RMS).

### 5.2. Altimeter Range

An altimeter operates by sending out a short pulse of radiation and measuring the time required for the pulse to return from the sea surface. This measurement, called the altimeter range, gives the distance between the instrument and the sea surface, provided that the velocity of the propagation of the pulse and the precise arrival time are known. The dual frequency altimeter on OSTM/Jason-2 performs range measurements at the Ku and C band frequencies (ku/range and c/range), enabling measurements of the range and the total electron content (see discussion below on ionosphere). While both range measurements are provided on the GDR, the Ku band range measurement has much higher accuracy than the C band measurement.

The range reported on the OSTM/Jason-2 (O)(I)GDR has already been corrected for a variety of calibration and instrument effects, including calibration errors, pointing angle errors, center of gravity motion, and terms related to the altimeter acceleration such as Doppler shift and oscillator drift. The sum total of these corrections also appears on the GDR for each of the Ku and C band ranges (see `range_cor_ocean_net_instr`, `range_cor_ocean_mle3_net_instr` and `range_cor_adaptive_net_instr`).

### 5.3. Geoid

The geoid is an equipotential surface of the Earth's gravity field that is closely associated with the location of the mean sea surface. The reference ellipsoid is a bi-axial ellipsoid of revolution. The center of the ellipsoid is ideally at the center of mass of the Earth although the center is usually placed at the origin of the reference frame in which a satellite orbit is calculated and tracking station positions given. The separation between the geoid and the reference ellipsoid is the geoid undulation (see geoid parameter).

The geoid undulation, over the entire Earth, has a root mean square value of 30.6 m with extreme values of approximately 83 m and -106 m. Although the geoid undulations are primarily long wavelength phenomena, short wavelength changes in the geoid undulation are seen over seamounts, trenches, ridges, etc., in the oceans. The calculation of a high resolution geoid requires high resolution surface gravity data in the region of interest as well as a potential coefficient model that can be used to define the long and medium wavelengths of the Earth's gravitational field. Surface gravity data are generally only available in certain regions of the Earth and spherical harmonic expansions of the Earth's gravitational potential are usually used to define the geoid globally. Currently, such expansions are available to degree 360 and in some cases higher.

For ocean circulation studies, it is important that the long wavelength part of the geoid be accurately determined.

### 5.4. Mean Sea Surface

A Mean Sea Surface (MSS) represents the position of the ocean surface averaged over an appropriate time period to remove annual, semi-annual, seasonal, and spurious sea surface height signals. A MSS



is given as a grid with spacing consistent with the altimeter and other data used in the generation of the grid values. The MSS grid can be useful for data editing purposes, for the calculation of along track and cross track geoid gradients, for the calculation of gridded gravity anomalies, for geophysical studies, for a reference surface to which sea surface height data from different altimeter missions can be reduced, etc. The OSTM/Jason-2 GDR provides two global MSS model that is generated from multiple satellite altimetry missions (see `mean_sea_surface_cnescls` and `mean_sea_surface_dtu`).

Longer time spans of data that become available in the future, along with improved data handling techniques will improve the current MSS models. Care must be given to the retention of high frequency signal and the reduction of high frequency noise.

## 5.5. Mean Dynamic Topography

A Mean Dynamic Topography (MDT) represents the Mean Sea Surface referenced to a geoid and corrected from geophysical effects. A MDT is given as a grid with spacing consistent with the altimeter and other data used in the generation of the grid values. The MDT provides the absolute reference surface for the ocean circulation. The OSTM/Jason-2 GDR provides a global MDT model that is a combined product recovering several years based on GRACE mission, altimetry and in situ data (hydrologic and drifters data).

## 5.6. Geophysical Corrections

The atmosphere and ionosphere slow the velocity of radio pulses at a rate proportional to the total mass of the atmosphere, the mass of water vapor in the atmosphere, and the number of free electrons in the ionosphere. In addition, radio pulses do not reflect from the mean sea level but from a level that depends on wave height and wind speed. The errors due to these processes cannot be ignored and must be removed. Discussions of these effects are given in *Chelton et al.* [2001].

### 5.6.1. Troposphere (dry and wet)

The propagation velocity of a radio pulse is slowed by the "dry" gases and the quantity of water vapor in the Earth's troposphere. The "dry" gas contribution is nearly constant and produces height errors of approximately -2.3 m. The water vapor in the troposphere is quite variable and unpredictable and produces a height calculation error of -6 cm to -40 cm. However, these effects can be measured or modeled as discussed below.

#### 5.6.1.1. Dry Troposphere

The gases in the troposphere contribute to the index of refraction. In detail, the refractive index depends on pressure and temperature. When hydrostatic equilibrium and the ideal gas law are assumed, the vertically integrated range delay is a function only of the surface pressure, see *Chelton et al.* [2001]. The dry meteorological tropospheric range correction is principally equal to the surface pressure multiplied by -2.277mm/mbar, with a small adjustment also necessary to reflect a small latitude dependence (see Saastamoinen [1972] ).

$$\text{model\_dry\_tropo\_cor\_measurement\_altitude} = -2.277 * P_{\text{atm}} * [1 + 0.0026 * \cos(2 * \text{phi})]$$

where  $P_{\text{atm}}$  is surface atmospheric pressure at the measurement\_altitude in mbar, phi is latitude, and `model_dry_tropo_cor_measurement_altitude` is the dry troposphere correction in mm.

$$\text{model\_dry\_tropo\_cor\_zero\_altitude} = -2.277 P [1 + 0.0026 \cos(2 \text{ phi})] *_{\text{atm}} * + * *$$

where  $P_{\text{atm}}$  is surface atmospheric pressure at Mean Sea Level (MSL) in mbar, phi is latitude, and `model_dry_tropo_cor_zero_altitude` is the dry troposphere correction in mm at MSL altitude.

There is no straightforward way of measuring the nadir surface pressure from a satellite, so it is determined from the European Center for Medium Range Weather Forecasting (ECMWF) numerical weather prediction model. The uncertainty on the ECMWF atmospheric pressure products is somewhat dependent on location. Typical errors vary from 1 mbar in the northern Atlantic Ocean to a few mbars



in the southern Pacific Ocean. A 1-mbar error in pressure translates into a 2.3 mm error in the dry tropospheric correction.

The use of parameters estimated at DEM or measurement altitude for model dry and wet tropospheric corrections are recommended for hydrological application [Valladeau et al., 2015]

## 5.6.1.2. Wet Troposphere

The amount of water vapor present along the path length contributes to the index of refraction of the Earth's atmosphere. Its contribution to the delay of the radio pulse, the wet tropospheric delay, can be estimated by measuring the atmospheric brightness near the water vapor line at 22.2356 GHz and providing suitable removal of the background. The OSTM/Jason-2 Microwave Radiometer (AMR) measures the brightness temperatures in the nadir path at 18.7, 23.8 and 34.0 GHz: the water vapor signal is sensed by the 23.8 GHz channel, while the 18.7 GHz channel removes the surface emission (wind speed influence), and the 34 GHz channel removes other atmospheric contributions (cloud cover influence) [Keihm et al., 1995].

Measurements are combined to obtain the path delay in the satellite range measurement due to the water vapor content (see `rad_wet_tropo_cor` parameter).

The uncertainty is less than 1.2 cm RMS [e.g. Cruz Pol et al., 1998 and Ruf et al., 1994]. Since GDR-D product version, an improved near land wet path delay algorithm is applied to improve the performance up to the coast. The algorithm error when applied to the AMR is estimated to be less than 0.8 cm up to 15 km from land, less than 1.0 cm within 10 km from land, less than 1.2 cm within 5 km from land and less than 1.5 cm up to the coastline. This is estimated from detailed simulations and validated by comparisons with measured AMR data [Brown, 2009]. The radiometer surface type (see `rad_surface_type_flag` parameter) indicates the quality of this wet tropospheric correction.

The ECMWF numerical weather prediction model provides also a value for the wet tropospheric delay. An interpolated value from this model is included in the GDR, as a backup to the measurement from the AMR (see `model_wet_tropo_cor_measurement_altitude` and `model_wet_tropo_cor_zero_altitude`). This backup will prove useful when sun glint, land contamination, or anomalous sensor behavior makes the AMR measurement of the wet tropospheric delay unusable.

An interpolation quality flag is provided on the GDR to indicate the quality of this interpolation (see `meteo_zero_altitude_interp_qual`).

The use of parameters estimated at DEM or measurement altitude for model dry and wet tropospheric corrections are recommended for hydrological application [Valladeau et al., 2015]

## 5.6.2. Atmospheric Attenuation

See `sig0_cor_atm`

The radiometer solution is retrieved with the same approach detailed in the previous section.

When the radiometer is not available, a model solution is given. It is established from ECMWF analysis based on the equations provided by Keihm, 1995 for OGDR and IGDR, and Lillibridge et al., 2014 for GDR. In this later, pressure, temperature, humidity and cloud liquid water content ECMWF profiles are combined through polynomial relation to compute the model atmospheric attenuation at the measurement altitude.

A flag indicates whether the radiometer solution or the model solution is provided in `sig0_cor_atm` (see `sig0_cor_atm_source`)

## 5.6.3. Ionosphere

At the frequencies used by the Poseidon-3 altimeter, the propagation velocity of a radio pulse is slowed by an amount proportional to the density of free electrons of the Earth's ionosphere, also known as the total electron content (TEC). The retardation of velocity is inversely proportional to



frequency squared. For instance, it causes the altimeter to slightly over-estimate the range to the sea surface by typically 0.2 to 20 cm at 13.6 GHz. The amount varies from day to night (there are fewer free electrons at night), from summer to winter, and as a function of the solar cycle (there are fewer during solar minimum.) (For discussions on this correction, see *Chelton et al.* [2001], *Imel* [1994], and *Callahan* [1984].

Because this effect is dispersive, measuring the range at two frequencies allows it to be estimated. Under typical ocean conditions of 2-meter significant wave height, the Ku band ionospheric range correction determined from the dual frequency measurements from the altimeter is expected to have an accuracy of  $\pm 0.5$  cm (see `iono_corr_alt` parameter).

To reduce the noise a smoothed solution, derived from [*Imel*, 1994], is provided in the product (see `iono_cor_alt_filtered` parameter).

A backup ionospheric correction solution, derived from Global Ionosphere Maps (GIM), is provided in the GDR products. It may be used over non ocean surfaces (ice, land, etc.).

#### 5.6.4. Ocean Waves (sea state bias)

Unlike the preceding effects, sea-state effects are an intrinsic property of the large footprint radar measurements. The surface scattering elements do not contribute equally to the radar return; troughs of waves tend to reflect altimeter pulses better than do crests. Thus the centroid of the mean reflecting surface is shifted away from mean sea level towards the troughs of the waves. The shift, referred to as the electromagnetic (EM) bias, causes the altimeter to overestimate the range (see *Rodriguez et al.*, [1992]). In addition, a skewness bias also exists from the assumption in the onboard algorithms that the probability density function of heights is symmetric, while in reality it is skewed. Finally, there is a tracker bias, which is a purely instrumental effect. The sum of EM bias, skewness bias, and tracker bias is called 'sea state bias' (see `ku/sea_state_bias` and `c/sea_state_bias` parameters).

The accuracy of sea state bias models remains limited and continues to be a topic of research. The current most accurate estimates are obtained using empirical models derived from analyses of the altimeter data. The sea state bias is computed from a bilinear interpolation of a table of sea state biases versus significant wave height and wind speed, based on empirical fits (Labroue [2004]). For a typical significant wave height (SWH) of 2 meters, the sea state bias is about 10 cm, and the error (bias) in the sea state bias correction is approximately 1-2 cm. The noise of the sea state bias estimates depends mainly on the noise on the significant wave height estimates.

The 3D version consists in a table with a third input, the mean wave period provided by a wave model to better describe the local wave conditions and thus improves the sea state bias estimates [Tran et al, 2010].

#### 5.7. Rain Flag

---

Liquid water along the pulse's path reduces the energy returned to the altimeter, mainly at Ku band. In heavy rain, there are competing effects from attenuation and surface changes. The small-scale nature of rain cells tends to produce rapid changes in the strength of the echo as the altimeter crosses rain cells. Both effects degrade the performance of the altimeter. Data contaminated by rain are rare (most are located in the west equatorial pacific), flagged and should be ignored (see `rain_flag` parameter).

The rain flag on the OSTM/JASON-2 (O)(I)GDR is set if integrated liquid water content measured by the AMR is larger than a specified threshold, AND if the difference between the expected Ku-band backscatter coefficient (estimated from the C-band backscatter coefficient which is much less affected by rain) and the measured Ku-band backscatter coefficient, is larger than either a specified threshold or a specified multiple of the uncertainty in the expected Ku-band backscatter coefficient (see `rain_flag` parameter) [*Tournadre and Morland*, 1998] (and RD 3). Ku band backscatter coefficient used for the rain flag determination is issued from MLE3 retracking (`ku/sig0_ocean_mle3` and `c/sig0_ocean`).





Table 19 : List of classes defined for Jason-2 waveforms

- Class 1: Brownian echoes, mainly found in open ocean
- Class 2: peaky echoes, mainly encountered over narrow rivers, small lakes (smaller than the altimeter footprint) and water leads in sea ice regions
- Class 3: several peaks, corresponds to multiple reflection in the footprint, encountered over land or heterogeneous areas
- Class 4: strong peak with a very low trailing edge, corresponds to high reflective surfaces, often encountered on sea ice, most of the time over First Year Ice (FYI)
- Class 5: Brownian shape with a peak on the trailing edge, mainly found in coastal areas where the altimeter is close to the coast and a “bright point” is present in the footprint (but not at nadir)
- Class 6: Brownian shape with a peak on the leading edge or Brownian shape with a sharp trailing edge. Can be encountered over sea ice.
- Class 7: Brownian shape with a flat or increasing trailing edge. Can be found in rain cells or over land ice (it can also be a sign of a platform mispointing even if Jason-3 have good pointing performances).
- Class 8: peaky echo shifted at the end of the analysis window, mainly found on hydrology and land
- Class 9: trash echoes
- Class 10: Brownian shape with a high thermal noise level mainly found on land, land ice and sometimes on very heavy rain event
- Class 11: Double leading edge, can be encountered over land
- Class 12: shifted Brownian, can be found over land ice and hydrology (big lake with a non-optimal tracker command)
- Class 13: Brownian shape with a noisy leading edge
- Class 15: linear rise, can be found over land
- Class 18: linear decrease, can be found over land

The method used [Poisson 2020] is a neural network with one hidden layer of 23 neurons connecting 9 inputs parameters and 15 outputs classes (Inputs-Hidden-Outputs: 9-23-15). The neurons, within the hidden layer perform the same function. They simply calculate the weighted sum of inputs and weights, add the bias and execute an activation function (sigmoid). This final set of parameters for the neural network was analyzed and optimized in order to have the best performances of the network in term of prediction.

## 5.10. Tides

Tides are a significant contributor to the observed sea surface height [LeProvost, 2001]. While they are of interest in themselves, they have more variation than all other time-varying ocean signals. Since they are highly predictable, they are removed from the data in order to study ocean circulation. The T/P orbit was specifically selected (inclination and altitude) so that diurnal and semidiurnal tides would not be aliased to low frequencies.

There are several contributions to the tidal effect: the ocean tide, the load tide, the solid earth tide, the pole tide and the internal tide. The ocean tide, load tide, solid earth tide and internal tide are all related to luni-solar forcing of the earth, either directly as is the case of the ocean and solid earth tide, or indirectly as is the case with the load tide since it is forced by the ocean tide. The internal tide is forced by the ocean tide flow over sharp bottom topography. The pole tide is due to variations in the earth's rotation and is unrelated to luni-solar forcing.

OSTM/Jason-2 (O)(I)GDRs do not explicitly provide values for the pure ocean tide, but instead provide values for a quantity referred to as the geocentric ocean tide, which is the sum total of the ocean tide and the load tide. Values of the load tide that were used to compute the geocentric ocean tide are also explicitly provided, so the pure ocean tide can be determined by subtracting the load tide value from the geocentric ocean tide value. Note that the permanent tide is not included in either



the geocentric ocean tide or solid earth tide corrections that are provided on the OSTM/Jason-2 (O)(I)GDRs.

	Ocean Tide effects			Load Tide effects		
	short period	long period eq	long period non eq	short period	long period eq	long period non eq
<i>ocean_tide</i>	Yes	Yes	No	Yes	No	No
<i>load_tide</i>	No	No	No	Yes	No	Yes
<i>ocean_tide_eq</i>	No	Yes	No	No	No	No
<i>ocean_tide_non_eq</i>	No	No	Yes	No	No	Yes

Table 20 : Table of tide effects included in product variables

### 5.10.1. Geocentric Ocean Tide

As mentioned above, the geocentric ocean tide refers to the sum of the ocean tide and the load tide. The Jason-2 GDR provides two choices for the geocentric ocean tide, *ocean\_tide\_fes* and *ocean\_tide\_got*: each of them is computed as the sum of the ocean and load tides as predicted by a particular model for high frequencies (diurnal, semi-diurnal and non-linear tides with higher frequencies), and an equilibrium representation of the long-period ocean tides at all long-periods except for the zero frequency (constant) term which is not included. The two load tide values provided in the GDR, *load\_tide\_fes* and *load\_tide\_got*, provide the respective load tide values that were used to compute *ocean\_tide\_fes* and *ocean\_tide\_got*. As the ocean tide is set to zero on lakes and enclosed-seas, parameters *ocean\_tide\_fes* and *ocean\_tide\_got* are equal to the load tide value on these surfaces.

### 5.10.2. Long period Ocean Tide

The long-period ocean tides are a subject of continuing investigation. To first order, they can be approximated by an equilibrium representation. However, the true long-period ocean tide response is thought to have departures from an equilibrium response that increase with decreasing period. The two principal long-period ocean tide components, *Mf* and *Mm*, with fortnightly and monthly periods respectively, are known to have departures from an equilibrium response with magnitudes less than 1-2 cm.

The Jason-2 GDR explicitly provides a value for an equilibrium representation of the long-period ocean tide that includes all long-period tidal components excluding the permanent tide (zero frequency) component (see parameter *ocean\_tide\_eq*). Note that both geocentric ocean tide values on the (O)(I)GDR (*ocean\_tide\_fes* and *ocean\_tide\_got*) already include the equilibrium long-period ocean tide and should therefore not be used simultaneously.

The Jason-2 GDR also provides a parameter for a non-equilibrium representation of the long-period ocean tides (see parameter *ocean\_tide\_non\_eq*). This parameter is provided as a correction to the equilibrium long-period ocean tide model so that the total non-equilibrium long period ocean tide is formed as a sum of *ocean\_tide\_eq* and *ocean\_tide\_non\_eq*. The non-equilibrium long-period ocean tide provided in the Jason-3 (O)(I)GDR comes from FES2014b tide model, but the parameter *ocean\_tide\_non\_eq* can be used either with the *ocean\_tide\_fes* or the *ocean\_tide\_got*.

FES2014b model provides a dynamic solution for 6 long-period tidal frequencies: *Mf*, *Mm*, *MSqm*, *Mtm*, *Sa*, *Ssa*.

Parameter *ocean\_tide\_eq* is set to zero on lake and enclosed-seas, and the ocean tide part of the parameter *ocean\_tide\_non\_eq* is also set to zero on these surfaces.



## 5.10.3. Solid Earth Tide

The solid Earth responds to external gravitational forces similarly to the oceans. The response of the Earth is fast enough that it can be considered to be in equilibrium with the tide generating forces. Then, the surface is parallel with the equipotential surface, and the tide height is proportional to the potential. The two proportionality constants are the so-called Love numbers. It should be noted that the Love numbers are largely frequency independent, an exception occurs near a frequency corresponding to the K1 tide constituents due to a resonance in the liquid core [Wahr, 1985 and Stacey, 1977].

The OSTM/Jason-2 GDR computes the solid earth tide, or body tide, as a purely radial elastic response of the solid Earth to the tidal potential (see parameter `solid_earth_tide`.) The adopted tidal potential is the *Cartwright and Tayler* [1971] and *Cartwright and Edden* [1973] tidal potential extrapolated to the 2000 era, and includes degree 2 and 3 coefficients of the tidal potential. The permanent tide (zero frequency) term is excluded from the tidal potential that is used to compute the solid earth tide parameter for the OSTM/Jason-2 (O)(I)GDR. The elastic response is modeled using frequency independent Love numbers. The effects of the resonance in the core are accounted for by scaling the tide potential amplitude of the K1 tidal coefficient and some neighboring nodal terms by an appropriate scale factor.

## 5.10.4. Pole Tide

The pole tide is a tide-like motion of the ocean surface that is a response of both the solid Earth and the oceans to the centrifugal potential that is generated by small perturbations to the Earth's rotation axis. These perturbations primarily occur at periods of 433 days (called the Chandler wobble) and annual. These periods are long enough for the pole tide displacement to be considered to be in equilibrium with the forcing centrifugal potential. The OSTM/Jason-2 (O)(I)GDR provides a single field for the radial geocentric pole tide displacement of the ocean surface (see `pole_tide` parameter), and includes the radial pole tide displacement of the solid Earth and the oceans.

The pole tide is easily computed as described in Wahr [1985] and [Desai et al, 2017]. This new algorithm accounts for self-gravitation, loading, conservation of mass, and geocenter motion (spatial dependence). Over the oceans the pole tide includes the response of the solid earth, ocean, and loading effect; over land it includes only the impact on the solid earth and loading.

The mean pole variation model includes a bias AND a drift (temporal dependence), and the computed pole tide does NOT include the effects of the Earth's displacement response to that mean pole (drift).

Modeling the pole tide requires knowledge of proportionality constants, the so-called Love numbers, and a time series of perturbations to the Earth's rotation axis, a quantity that is now measured routinely with space techniques. Note that the pole tide on the IGDR and GDR may differ, since the pole tide on the GDR is computed with a more accurate time series of the Earth's rotation axis.

## 5.10.5. Internal Tide

Internal tides are baroclinic tides generated by the arrival of a barotropic tide flow on an underwater sharp topography pattern (seamount or shelfbreak region); they can reach amplitudes of several 10th of meters at the thermocline level and they have a signature of several cm at the surface with wavelengths about 50-250 km for the first mode and shorter wavelengths for higher modes.

To reach higher accuracy ocean signals using the Jason-2 GDR, we need to be able to separate all tides signals, including the small scale internal tides surface signatures, from other oceanic signals.

The global ocean tide models described in previous sections are barotropic tide models, so by essence they do not correct from the internal tides signature at the surface.

The Jason-2 GDR provides a value for the internal tide surface signature, taking into account the M2,S2,K1,O1 tidal frequencies from Zaron model [Zaron, 2019].

See parameter `internal_tide`.



---

## 5.11. Ocean response to atmospheric forcing

### 5.11.1. Inverted Barometer Correction

As atmospheric pressure increases and decreases, the sea surface tends to respond hydrostatically, falling or rising respectively. Generally, a 1-mbar increase in atmospheric pressure depresses the sea surface by about 1 cm. This effect is referred to as the inverse barometer (IB) effect.

The instantaneous IB effect on sea surface height in millimeters (see parameter `inv_bar_corr`) is computed from the surface atmospheric pressure,  $P_{atm}$  in mbar:

$$\text{inv\_bar\_corr} = -9.948 * (P_{atm} - P)$$

where  $P$  is the time varying mean of the global surface atmospheric pressure over the oceans.

The scale factor 9.948 is based on the empirical value [Wunsch, 1972] of the IB response at mid latitudes. Some researchers use other values. Note that the surface atmospheric pressure is also proportional to the dry tropospheric correction, and so the parameter `inv_bar_corr` approximately changes by 4 to 5 mm as `model_dry_tropo_corr` changes by 1 mm (assuming a constant mean global surface pressure). The uncertainty of the ECMWF atmospheric pressure products is somewhat dependent on location. Typical errors vary from 1 mbar in the northern Atlantic Ocean to a few mbars in the southern Pacific Ocean. A 1-mbar error in pressure translates into a 10 mm error in the computation of the IB effect.

Note that the time varying mean global pressure over the oceans,  $P$ , during the first eight years of the T/P mission had a mean value of approximately 1010.9 mbar, with an annual variation around this mean of approximately 0.6 mbar. However, the T/P data products provided a static inverse barometer correction referenced to a constant mean pressure of 1013.3 mbar.

$$\text{IB(T/P)} = -9.948 * (P_{atm} - 1013.3)$$

Sea surface heights that are generated after applying an inverse barometer correction referenced to a mean pressure of 1013.3 mbar are therefore approximately  $-9.948 * (1010.9 - 1013.3) = 23.9$  mm lower than those that are generated after applying an inverse barometer correction referenced to a time varying global mean pressure, and the difference between the two sea surface heights has an annual variation of approximately  $9.948 * 0.6 = 6$  mm.

### 5.11.2. Dynamic Atmospheric Correction

The Dynamic Atmospheric Correction (DAC) allows taking into account the dynamic response of the ocean to atmospheric forcing for high frequencies, and it can be used instead of the Inverted Barometer correction (`inv_bar_cor`). This new field `dac` provided in the Jason-3 (O)(I)GDR replaces the use of the sum of the formerly `hf_fluctuations_corr + inv_bar_corr`.

The ocean response to wind and pressure is mostly dynamic and is significantly energetic at short periods so that the static IB correction is not sufficient; several models approaches have been developed and showed that a barotropic model allows a good representation of this variability (Ponte 1991, Stammer et al. 1999, Mathers 2000, Tierney et al. 2000, Carrere 2003, Vinogradova and Ponte 2008).

The DAC is composed from the high frequencies of the barotropic ocean model MOG2D, forced by ECMWF operational wind and pressure fields and the low frequencies of the IB (Carrere and Lyard, 2003). The cut-off frequency is 20 days and corresponds to the Nyquist frequency of the reference TP/Jason altimeters which have a 10 days cycle. DAC is therefore capable of removing almost all the high-frequency dynamic signal forced by the atmosphere (pressure and wind) and aliased in the altimetric measurement, except the errors and uncertainties of the model.



---

## 5.12. Sigma 0

---

The backscatter coefficients, sigma0 Ku and C values (see parameters ku/sig0\_ocean and c/sig0\_ocean), reported on the GDR are corrected for atmospheric attenuation using ku/sig0\_cor\_atm and c/sig0\_cor\_atm.

## 5.13. Note that "nominal" sigma0 values are recorded on the Jason-3 data products. For the altimeter wind retrieval, a bias is applied to the provided sigma in order to get a 1-year period wind speed distribution form similar to the one observed by ERA5 model. Wind Speed

---

The model functions developed to date for altimeter wind speed have all been purely empirical. A wind speed is calculated through a mathematical relationship with the Ku-band backscatter coefficient and the significant wave height (see wind\_speed\_alt) using the Gourrion approach [Gourrion *et al.*, 2002] and Collard's model computed from Jason-1 data [Collard, 2005].

A calibration bias is applied on Jason-2 Ku-band backscatter coefficient (0.27dB for MLE4 and 0.109 dB for MLE3). The wind speed model function is evaluated for 10 meter above the sea surface, and is considered to be accurate to 2 m/s.

A radiometer derived wind speed is also computed through an empirical relationship to brightness temperatures measured by the AMR [Keihm *et al.*, 1995] (see wind\_speed\_rad). The coefficients of this relationship have been determined from the regression of island radiosonde data computations combined with seasonal and latitude dependent wind speed statistics.

Finally, a 10-meter (above surface) wind vector (in east-west and north-south directions) is also provided on the OSTM/Jason-2 (O)(I)GDR (see parameters wind\_speed\_model\_u and wind\_speed\_model\_v). This wind speed vector is determined from an interpolation of the ECMWF model. The best accuracy for the wind vector varies from about 2 m/s in magnitude and 20 degrees in direction in the northern Atlantic Ocean, to more then 5 m/s and 40 degrees in the southern Pacific Ocean.

## 5.14. Bathymetry Information

---

The OSTM/Jason-2 GDR provides a parameter bathymetry that gives the ocean depth or land elevation of the data point. Ocean depths have negative values, and land elevations have positive values. This parameter is given to allow users to make their own "cut" for ocean depth.



## 6. Data description

### 6.1. (O)(I)GDR content

The main characteristics of (O)(I)GDR products are summarized in the following table.

Features	OGDR	IGDR	GDR
<b>Primary Goal</b>	To provide wind/wave data to meteorological users. Also designed to provide altimeter range, environmental and geophysical corrections together with a real-time orbit in order to make NRT SSHA available to ocean users	To provide sea surface height data to operational oceanography users (with a more accurate orbit and additional environmental / geophysical corrections w.r.t. OGDR)	To fulfill the project science objectives (AD 2)
<b>Content</b>	Geophysical level 2 product (Poseidon-3/AMR), including waveforms retracking		
	+ available environmental and geophysical corrections	+ all the environmental and geophysical corrections (preliminary for some of them)	+ all the environmental and geophysical corrections (precise)
<b>Orbit</b>	5 cm DORIS navigator	2.5 cm MOE (processed DORIS+GPS data)	1.5 cm POE (processed DORIS and/or GPS and/or laser data)
<b>Delivery delay (after data acquisition)</b>	Near-Real Time	Off-Line	Off-Line
	3-5 hours	2 calendar days	90 days
<b>Validation</b>	Not fully validated (elementary and automatic controls only)		Fully validated (in depth validation performed on a cycle basis before delivery)
<b>Validation by Experts</b>	No		Yes (NASA/JPL and CNES/SALP)
<b>Structure</b>	Segment (see 0)	Pole to pole pass	
<b>Ground Processing Centre</b>	NOAA and EUMETSAT	CNES	

**Table 21** : Main characteristics of (O)(I)GDR products

Please note that contrary to previous standard, OGDR and IGDR are not available for “F” standard which is a No Time Critical standard only.

For more information about (O)(I)GDR differences, please refer to previous version of this document (Issue 1)

### 6.2. Datasets

OSTM/Jason-2 OGDR, IGDR and GDR products , accounting for Jason-1 heritage, are split into three data sets :

- “SSHA” data set : One file, limited to 1Hz sampling values
- “GDR” data set : One file containing 1Hz and 20Hz values
- “SGDR” data set : One file containing 1Hz, 20hz and waveforms values



---

## 6.3. Product Description

---

The netCDF data format has been chosen to store the different data sets (one file per data set). This format is extremely flexible, self describing and has been adopted as a de-facto standard for many operational oceanography systems. What's more, the files follow the Climate and Forecast NetCDF conventions CF-1.7 because these conventions provide a practical standard for storing. A netCDF file contains **dimensions**, **variables**, **groups**, and **attributes**, which all have both a name by which they are identified. These components can be used together to capture the meaning of data and relations among data fields in an array-oriented data set.

Full Product description (format, global attributes, groups, dimensions, variables names and their attributes) is provided in [AD9]

---

## 6.4. Software

---

This section lists some software that may be used to browse and use data from SSHA, GDR and SGDR data sets.

### 6.4.1. Software provided with netCDF : “ncdump”

« ncdump » converts netCDF files to ASCII form (CDL)

See <https://www.unidata.ucar.edu/software/netcdf/workshops/2011/utilities/index.html>

The main options are the following :

- h Show only the header information in the output, that is the declarations of dimensions, variables, and attributes but no data values for any variables
- c Show the values of coordinate variables (variables that are also dimensions) as well as the declarations of all dimensions, variables, and attribute values
- v *var1,...,varn* The output will include data values for the specified variables, in addition to the declarations of all dimensions, variables, and attributes
- x *var1,...,varn* Output XML (NcML) instead of CDL. The NcML does not include data values

### 6.4.2. Additional general software

#### 6.4.2.1. ncbrowse

“ncBrowse” is a Java application that provides flexible, interactive graphical displays of data and attributes from a wide range of netCDF data file conventions.

See <http://www.pmel.noaa.gov/epic/java/ncBrowse/>

#### 6.4.2.2. netCDF Operator (NCO)

The netCDF Operators, or “NCO”, are a suite of programs known as **operators**. Each operator is a standalone, command line program which is executed at the UNIX shell-level, like, e.g., `ls` or `mkdir`. The operators take netCDF files as input, then perform a set of operations (e.g., deriving new data, averaging, hyperslabbing, or metadata manipulation) and produce a netCDF file as output. The operators are primarily designed to aid manipulation and analysis of gridded scientific data. The single command style of NCO allows users to manipulate and analyze files interactively and with simple scripts, avoiding the overhead (and some of the power) of a higher level programming environment.

See <http://nco.sourceforge.net/>

### 6.4.3. Additional specific software : “BRAT”

The “Basic Radar Altimetry Toolbox” is a collection of tools and tutorial documents designed to facilitate the use of radar altimetry data. It is able to read most distributed radar altimetry data from all the satellites, to do some processing, data editing and statistic over them, and to visualize the



---

results. The Basic Radar Altimetry Toolbox is able to read ERS-1 and 2, TOPEX/Poseidon, GEOSAT Follow-on, Jason-1, ENVISAT, OSTM/Jason-2 and CRYOSAT missions altimetry data from official data centers (ESA, NASA/JPL, CNES/AVISO, NOAA), and this for different processing levels, from level 1B (Sensor Geophysical Data Record) to level 3/4 (gridded merged data).

See [http://www.altimetry.info/html/data/toolbox\\_en.html](http://www.altimetry.info/html/data/toolbox_en.html)



## Annexe A - References

Benada, J. R., 1997, "PO.DAAC Merged GDR (TOPEX/POSEIDON) Generation B User's Handbook", Version 2.0, JPL D-11007.

Berry, P. A. M., R. Smith, and J. Benveniste. 2019. Altimeter Corrected Elevations, Version 2 (ACE2). Palisades, NY: NASA Socioeconomic Data and Applications Center (SEDAC). <https://doi.org/10.7927/H40G3H78> ; <https://sedac.ciesin.columbia.edu/data/set/dedc-ace-v2>

Bonnefond, P., P. Exertier, O. Laurain, Y. Menard, A. Orsoni, E. Jeansou and G. Jan, 2002, "Absolute calibration of Jason-1 and TOPEX/POSEIDON altimeters in Corsica (abstract)", Jason-1/TOPEX/POSEIDON Science Working Team, New Orleans, LA, USA.

Brenner, A. C., C. J. Koblinsky, and B. D. Beckley, 1990, A Preliminary Estimate of Geoid-Induced Variations in Repeat Orbit Satellite Altimeter Observations, *J. Geophys. Res.*, 95(c3), 3033-3040.

Brown, S., 2009, A Novel Near-Land Radiometer Wet Path Delay Retrieval Algorithm: Application to the Jason-2/OSTM Advanced Microwave Radiometer", submitted to IEEE Trans. Geosci. Rem. Sens.

Callahan, P. S., 1984, Ionospheric Variations affecting Altimeter Measurements: A brief synopsis *Marine Geodesy*, 8, 249-263.

Cartwright, D. E. and R. J. Tayler, 1971, New computations of the tide-generating potential, *Geophys. J. R. Astr. Soc.*, 23, 45-74.

Cartwright, D. E. and A. C. Edden, 1973, Corrected tables of tidal harmonics, *Geophys. J. R. Astr. Soc.*, 33, 253-264.

Chambers et al., 1998, Reduction of geoid gradient error in ocean variability from satellite altimetry, *Marine Geodesy*, 21, 25-40.

Chelton, D. B., J. C. Ries, B. J. Haines, L. L. Fu, and P. S. Callahan, 2001, "Satellite Altimetry", *Satellite Altimetry and Earth Sciences*, ed. L.L. Fu and A. Cazenave, pp. 1-131.

Collard, F., 2005: Algorithmes de vent et période moyenne des vagues JASON à base de réseaux de neurons. BO-021-CLS-0407-RF, Boost Technologies, 33 pp.

Cruz Pol, S. L., C. S. Ruf, and S. J. Keihm, 1998, Improved 20-32 GHz atmospheric absorption model, *Radio Science*.

Desai S. , Wahr J., Beckley B., 2015, Revisiting the pole tide for and from satellite altimetry, *Journal of Geodesy* volume 89, pages1233-1243  
Desai S. D. and Ries J.C., 2017, "Conventional model update for rotational deformation," in Fall AGU Meeting, New Orleans, LA, 2017

Gaspar, P., F. Ogor, P. Y. Le Traon and O. Z. Zanife, 1994, Estimating the sea state of the TOPEX and POSEIDON altimeters from crossover differences, *J. Geophys. Res.*, 99, 24981-24994.

Gaspar, P., F. Ogor and C. Escoubes, 1996, Nouvelles calibration et analyse du biais d'état de mer des altimètres TOPEX et POSEIDON, Technical note 96/018 of CNES Contract 95/1523.

Gourrion, J., Vandemark D., Bailey S., Chapron B., Gommenginger G. P., Challenor P. G., and Srokosz M. A., 2002: A two-parameter wind speed algorithm for Ku-band altimeters. *J. Atmos. Oceanic Technol.*, 19, 2030-2048

Haines, B., D. Kubitschek, G. Born and S. Gill, 2002, "Monitoring Jason-1 and TOPEX/POSEIDON from an offshore platform: The Harvest experiment (abstract)", Jason-1/TOPEX/POSEIDON Science Working Team, New Orleans, LA, USA.

Imel, D., 1994, Evaluation of the TOPEX dual-frequency ionosphere correction, *J. Geophys. Res.*, 99 (c12), pp 24895-24906.



- Keihm, S. J., M. A. Janssen, and C. S. Ruf, 1995, TOPEX/POSEIDON microwave radiometer (TMR): III. Wet troposphere range correction algorithm and pre-launch error budget, *IEEE Trans. Geosci. Remote Sensing*, 33, 147-161.
- Labroue S., P. Gaspar, J. Dorandeu, O.Z. Zanife, F. Mertz, P. Vincent and D. Choquet, 2004: Non parametric estimates of the sea state bias for the Jason-1 radar altimeter. *Marine Geodesy* 27 (3-4), 453-481.
- Le Provost, C., 2001, "Ocean Tides", *Satellite Altimetry and Earth Sciences*, ed. L.L. Fu and A. Cazenave, pp. 267-303.
- Le Provost, C., F. Lyard, M. L. Genco, F. Lyard, P. Vincent, and P. Canceil, 1995, Spectroscopy of the world ocean tides from a finite element hydrodynamic model, *J. Geophys. Res.*, 99, 24777-24797.
- Lefèvre F., F. Lyard, C. Le Provost and E.J.O Shrama, Fes99 : a global tide finite element solution assimilating tide gauge and altimetric information, *J. Atm. Oceano. Tech.*, submitted, 2001.
- Lemoine, F. G. et al., 1998, The Development of the joint NASA GSFC and NIMA Geopotential Model EGM96, NASA/TP-1998-206861, 575 pp.
- Lillibridge, J., Scharroo, R., Abdalla, S., & Vandemark, D. , 2014: One-and two-dimensional wind speed models for ka-band altimetry, *Journal of Atmospheric and Oceanic Technology*, 31(3), 630-638. <http://doi.org/10.1175/JTECH-D-13-00167.1>
- Pavlis, N. and R. H. Rapp, 1990, The development of an isostatic gravitational model to degree 360 and its use in global gravity modeling, *Geophys. J. Int.*, 100, 369-378.
- Poisson et al. 2020, Classification des échos Jason-3, SALP-NT-MA-EA-23416-CLS, 2020,Mar.18
- Rapp, R. H. et al., 1991, Consideration of Permanent Tidal Deformation in the Orbit Determination and Data Analysis for the TOPEX/POSEIDON Mission, NASA Tech. Memorandum 100775, Goddard Space Flight Center, Greenbelt, MD.
- Rapp, R. H., Y. M. Wang, and N. K. Pavlis, 1991, The Ohio State 1991 geopotential and Sea Surface Topography Harmonic Coefficient Models, Rpt. 410, Dept. of Geodetic Science and Surveying, The Ohio State University, Columbus, OH.
- Ray, R. D., 1999, A global ocean tide model from TOPEX/POSEIDON altimetry: GOT99.2, NASA Tech. Memorandum 1999-209478, Goddard Space Flight Center, Greenbelt, MD.
- Ray R D and Ponte R M, 2003 Barometric tides from ECMWF operational analyses, *Annales Geophysicae*, 21: 1897-1910, 2003.
- Rio M.-H., F. Hernandez, 2004, A mean dynamic topography computed over the world ocean from altimetry, in situ measurements, and a geoid model, *J. Geophys. Res.*, 109, C12032.
- Rio, M.-H., Schaeffer, P., Lemoine, J.-M., Hernandez, F. (2005). "Estimation of the ocean Mean Dynamic Topography through the combination of altimetric data, in-situ measurements and GRACE geoid: From global to regional studies." Proceedings of the GOCINA international workshop, Luxembourg.
- Rio M.-H., A. Pascual, P.-M. Poulain, M. Menna, B. Barceló, and J. Tintoré, 2014, Computation of a new mean dynamic topography for the Mediterranean Sea from model outputs, altimeter measurements and oceanographic in situ data. *Ocean Science*.
- Rodriguez, E., Y. Kim, and J. M. Martin, 1992, The effect of small-wave modulation on the electromagnetic bias, *J. Geophys. Res.*, 97(C2), 2379-2389.
- Ruf, C., S. Keihm, B. Subramanya, and M. Janssen, 1994, TOPEX/POSEIDON microwave radiometer performance and in-flight calibration, *J. Geophys. Res.*, 99, 24915-24926.
- Saastamoinen, J., 1972: Atmospheric correction for the troposphere and stratosphere in radio ranging of satellites, *Geophys. Monogr.*, 15, American Geophysical Union, Washington D.C.
- Sandwell, D. T., and W. H. F. Smith, 2013 : Slope Correction for Ocean Radar Altimetry, *Journal of Geodesy*, DOI 10.1007/s00190-014-0720-1, 2013. <http://topex.ucsd.edu/sandwell/publications/149.pdf>  
[ftp://topex.ucsd.edu/pub/global\\_VD\\_1min/DH.grd](ftp://topex.ucsd.edu/pub/global_VD_1min/DH.grd)



- Smith, W. H. F. and D. T. Sandwell, 1994, Bathymetric prediction from dense satellite altimetry and sparse shipboard bathymetry, *J. Geophys. Res.*, 99, 21803-21824.
- Stacey, F. D., 1977, *Physics of the Earth*, second ed. J. Wiley, 414 pp.
- Stammer, D., C. Wunsch, and R. M. Ponte, 2000, De-aliasing of global high frequency barotropic motions in altimeter observations, *Geophys. Res. Lett.*, 27, 1175-1178.
- Tapley, B. D. et al., 1994, Accuracy Assessment of the Large Scale Dynamic Ocean Topography from TOPEX/POSEIDON Altimetry, *J. Geophys. Res.*, 99 (C12), 24, 605-24, 618.
- Tierney, C., J. Wahr, F. Bryan, and V. Zlotnicki, 2000, Short-period oceanic circulation: implications for satellite altimetry, *Geophys. Res. Lett.*, 27, 1255-1258.
- Thibaut P., Piras F., Roinard H., Guerou A., Boy F., Maraldi C., Bignalet-Cazalet F., Dibarbouré G., Picot N., 2021 BENEFITS OF THE “ADAPTIVE RETRACKING SOLUTION” FOR THE JASON-3 GDR-F REPROCESSING CAMPAIGN, IGARSS 2021
- Tournadre, J., and J. C. Morland, 1998, The effects of rain on TOPEX/POSEIDON altimeter data, *IEEE Trans. Geosci. Remote Sensing*, 35, 1117-1135.
- Tran, N., D. Vandemark, S. Labroue, H. Feng, B. Chapron, H. L. Tolman, J. Lambin, and N. Picot, 2010 : “Sea state bias in altimeter sea level estimates determined by combining wave model and satellite data”, *J. Geophys. Res.*, 115, C03020, doi:10.1029/2009JC005534.
- Tran N., D. Vandemark, E.D. Zaron, P. Thibaut, G. Dibarbouré, and N. Picot , 2019: “Assessing the effects of sea-state related errors on the precision of high-rate Jason-3 altimeter sea level data”, *Advances in Space Research / special issue “ 25 Years of Progress in Radar Altimetry”*, doi:10.1016/j.asr.2019.11.034
- Valladeau, G., Thibaut, P., Picard, B., Poisson, J. C., Tran, N., Picot, N., & Guillot, A., 2015: *Using SARAL/AltiKa to Improve Ka-band Altimeter Measurements for Coastal Zones, Hydrology and Ice: The PEACHI Prototype*, *Marine Geodesy*, 38, 124-142. <http://doi.org/10.1080/01490419.2015.1020176>
- Watson, C., R. Coleman, N. White, J. Church and R. Govind, 2002, "In-situ calibration activities in Bass Strait, Australia (abstract)", Jason-1/TOPEX/POSEIDON Science Working Team, New Orleans, LA, USA.
- Witter, D. L., and D. B. Chelton, 1991, A Geosat altimeter wind speed algorithm and a method for altimeter wind speed algorithm development, *J. Geophys. Res.*, 96, 8853-8860.
- Wunsch, C., 1972, Bermuda sea level in relation to tides, weather and baroclinic fluctuations, *Rev. Geophys. Space Phys.*, 10, 1-49.
- Yi, Y., 1995, Determination of Gridded Mean Sea Surface from TOPEX, ERS-1 and GEOSAT Altimeter Data, Rpt. 434, Dept. of Geodetic Science and Surveying, The Ohio State University, Columbus, 9363-9368.
- Zaron E. D, 2019, Baroclinic tidal sea level from exact-repeat mission altimetry. *Journal of Physical Oceanography*, 49(1):193-210, 2019; "HRET\_v8.1": <http://web.cecs.pdx.edu/~zaron/pub/HRET.html>
- Zlotnicki, V., 1994, Correlated environmental corrections in TOPEX/POSEIDON, with a note on ionospheric accuracy, *J. Geophys. Res.*, 99, 24907-24914.



## Annexe B - List of acronyms

AD	Applicable Document
AGC	Automatic Gain Control
AMR	Advanced Microwave Radiometer
AVISO	Archivage, Validation et Interprétation des données des Satellites Océanographiques
BRAT	Basic Radar Altimetry Toolbox
BUFR	<b>B</b> inary <b>U</b> niversal <b>F</b> orm for the <b>R</b> epresentation of Meteorological data
CLIVAR	Climate Variability and Predictability program
CLS	Collecte Localisation Satellites
CNES	Centre National d'Etudes Spatiales
DIODE	Détermination Immédiate d'Orbite par Doris Embarque
DORIS	Détermination d'Orbite et Radiopositionnement Intégrés par Satellite
DTM	Digital Terrain Model
ECMWF	European Center for Medium range Weather Forecasting
EGM	Earth Gravity Model
EM	ElectroMagnetic
EUMETSAT	European Organisation for the Exploitation of Meteorological Satellites
FES	Finite Element Solution
FFT	Fast Fourier Transform
GDR	Geophysical Data Records
GIM	Global Ionosphere Maps
GODAE	Global Ocean Data Assimilation Experiment
GPS	Global Positioning System
GTS	Global Telecommunications System
HF	High Frequency
IB	Inverse Barometer
IGDR	Interim Geophysical Data Records
JAXA	Japan Aerospace Exploration Agency
JGM	Joint Gravity Model
JPL	Jet Propulsion Laboratory
LPT	Light Particle Telescope
MDT	Mean Dynamic Topography
MLE	Maximum Likelihood Estimator
MSS	Mean Sea Surface
NASA	National Aeronautics and Space Administration
NetCDF	Network Common Data Form
NOAA	National Oceanic and Atmospheric Administration
NRT	Near Real Time
NWP	Numerical Weather Prediction
OGDR	Operational Geophysical Data Records
OSTM	Ocean Surface Topography Mission
OSU	Ohio State University
PO.DAAC	Physical Oceanography Distributed Active Archive Center
POD	Precision Orbit Determination
POE	Precision Orbit Ephemerides
PROTEUS	Plate Forme Reconfigurable pour l'Observation de la Terre, les telecommunications et les Utilisations Scientifiques
RD	Reference Document
RMS	Root Mean Square
RSS	Root Sum Square
SLA	Sea Level Anomaly
SLR	Satellite Laser Ranging
SSALTO	Segment Sol multimissions d'ALTimétrie, d'Orbitographie et de localisation précise
SSB	Sea State Bias
SSH	Sea Surface Height
SSHA	Sea Surface Height Anomaly
SWH	Significant Wave Height



# OSTM/Jason-2 Products Handbook

Iss :2.0- date : Apr 15th , 2025



67

---

T/P	Topex/Poseidon
T2L2	Time Transfer by Laser Link
TBC	To be confirmed
TBD	To be defined
TEC	Total Electron Content
TRSR	Turbo Rogue Space Receiver
UTC	Universal Time Coordinated
WMO	World Meteorological Organisation



## Annexe C - Contacts

### CNES

18, avenue Edouard Belin  
F-31401 Toulouse Cedex 9

Web : [www.cnes.fr](http://www.cnes.fr)

### AVISO+ User Service Helpdesk:

8-10 rue Hermès  
F-31520 Ramonville-St-Agne, France

Fax : +33 (0) 561 393 782  
Web : [www.avis.altimetry.fr](http://www.avis.altimetry.fr)  
e-mail : [avis@altimetry.fr](mailto:avis@altimetry.fr)

### EUMETSAT

D-64295 Darmstadt, Germany

Web : [www.eumetsat.int](http://www.eumetsat.int)

### User Service Helpdesk:

Tel : +49 6151 807 366/377  
Fax : +49 6151 807 379  
e-mail : [ops@eumetsat.int](mailto:ops@eumetsat.int)

### NOAA

### User Service Helpdesk:

Tel : +1 301-713-3277  
e-mail : [NODC.services@noaa.gov](mailto:NODC.services@noaa.gov)